THE JOURNAL OF BIOLOGICAL CHEMISTRY VOL. 285, NO. 13, pp. 9667–9682, March 26, 2010
© 2010 by The American Society for Biochemistry and Molecular Biology, Inc. Printed in the U.S.A.

Importance of Membrane Structural Integrity for RPE65 Retinoid Isomerization Activity*

Received for publication, September 9, 2009, and in revised form, December 21, 2009 Published, JBC Papers in Press, January 25, 2010, DOI 10.1074/jbc.M109.063941

Marcin Golczak[‡1], Philip D. Kiser[‡1,2], David T. Lodowski[‡2], Akiko Maeda[§], and Krzysztof Palczewski[‡3]

From the Departments of [‡]Pharmacology and [§]Ophthalmology and Visual Sciences, School of Medicine, Case Western Reserve University, Cleveland, Ohio 44106

Regeneration of visual chromophore in the vertebrate visual cycle involves the retinal pigment epithelium-specific protein RPE65, the key enzyme catalyzing the cleavage and isomerization of all-*trans*-retinyl fatty acid esters to 11-*cis*-retinol. Although RPE65 has no predicted membrane spanning domains, this protein predominantly associates with microsomal fractions isolated from bovine retinal pigment epithelium (RPE). We have re-examined the nature of RPE65 interactions with native microsomal membranes by using extraction and phase separation experiments. We observe that hydrophobic interactions are the dominant forces that promote RPE65 association with these membranes. These results are consistent with the crystallographic model of RPE65, which features a large lipophilic surface that surrounds the entrance to the catalytic site of this enzyme and likely interacts with the hydrophobic core of the endoplasmic reticulum membrane. Moreover, we report a critical role for phospholipid membranes in preserving the retinoid isomerization activity and physical properties of RPE65. Isomerase activity measured in bovine RPE was highly sensitive to phospholipase A_2 treatment, but the observed decline in 11-*cis*-retinol production did not directly reflect inhibition by products of lipid hydrolysis. Instead, a direct correlation between the kinetics of phospholipid hydrolysis and retinoid isomerization suggests that the lipid membrane structure is critical for RPE65 enzymatic activity. We also provide evidence that RPE65 operates in a multiprotein complex with retinol dehydrogenase 5 and retinal G protein-coupled receptor in RPE microsomes. Modifications in the phospholipid environment affecting interactions with these protein components may be responsible for the alterations in retinoid metabolism observed in phospholipid-depleted RPE microsomes. Thus, our results indicate that the enzymatic activity of native RPE65 strongly depends on its membrane binding and phospholipid environment.

In vertebrates, the perception of light is preceded by a quantum event in which a photon of light hits the 11-*cis*-retinylidene chromophore of rhodopsin in the retina. Photoisomerization of this chromophore to its all-*trans* isomer results in activation of rhodopsin triggering a cascade of signal transduction events (summarized in Ref. 1). This process simultaneously leads to loss of photoreceptor light sensitivity making continuous regeneration of 11-*cis*-retinal a requirement to sustain vision. The visual (retinoid) cycle is the fundamental series of reactions responsible for regeneration of the visual chromophore that occurs in photoreceptors and the retinal pigment epithelium (RPE)[4] (summarized in Ref. 2). The key component of this enzymatic cycle is the RPE-specific microsomal membrane protein known as RPE65 (3–5). The importance of RPE65 in the retinoid cycle is underscored by the metabolic dysfunction found in $Rpe65^{-/-}$ mice, which is characterized by complete lack of 11-*cis*-retinoid production accompanied by accumulation of the all-*trans*-retinyl esters, which serve as substrates for this enzyme (6). In humans, certain RPE65 mutations cause the hereditary childhood blinding disease known as Leber congenital amaurosis as well as the less severe retinitis pigmentosa (7–9).

Lipid membranes are a preferred environment for enzymes that metabolize hydrophobic substrates such as retinoids. Thus, critical enzymatic activities required for visual chromophore regeneration, *i.e.* formation of retinyl esters by lecithin:retinol acyltransferase (LRAT), retinoid isomerization catalyzed by RPE65, and retinol oxidation facilitated by a family of retinol dehydrogenases, are all associated with the microsomal fraction isolated from the RPE (5, 10, 11). Although the molecular basis of membrane association for LRAT and some of the retinol dehydrogenases has been elucidated, the mechanism by which RPE65 binds membranes and the role of specific phospholipids in its enzymatic activity are matters of debate. Understanding the nature of RPE65 membrane binding has been complicated by the observation that a subset of total RPE65 is apparently soluble and by the results of hydropathy plots of the

* This work was supported, in whole or in part, by National Institutes of Health Grants EY019478, EY009339, K08 EY019031, and P30 EY11373. This work was also supported by Foundation Fighting Blindness, Research to Prevent Blindness Foundation, and Ohio Lions Eye Research Foundation.

The atomic coordinates and structure factors (code 3KVC) have been deposited in the Protein Data Bank, Research Collaboratory for Structural Bioinformatics, Rutgers University, New Brunswick, NJ (http://www.rcsb.org/).

[1] Both authors contributed equally to this work.

[2] Supported by National Institutes of Health Visual Sciences Training Program Grant T32EY007157 from NEI.

[3] To whom correspondence should be addressed: Dept. of Pharmacology, School of Medicine, Case Western Reserve University, 10900 Euclid Ave., Cleveland, OH 44106-4965. Tel.: 216-368-4631; Fax: 216-368-1300; E-mail: kxp65@case.edu.

[4] The abbreviations used are: RPE, retinal pigment epithelium; BMH, bis(maleimido)hexane; C_8E_4, octyltetraoxyethylene; CAPS, *N*-cyclohexyl-3-aminopropanesulfonate; CHAPS, 3-(3-cholamidopropyl)dimethylammonio]-1-propanesulfonate; CRALBP, cellular retinaldehyde-binding protein; LRAT, lecithin:retinol acyltransferase; lyso-PC, 1-acyl-2-hydroxy-*sn*-glycero-3-phosphocholine; lyso-PE, 1-acyl-2-hydroxy-*sn*-glycero-3-phosphoethanolamine; PC, phosphatidylcholine; PE, phosphatidylethanolamine; PLA_2, phospholipase A_2; RGR, retinal G protein-coupled receptor; BisTris propane, 1,3-bis[tris(hydroxymethyl)methylamino]propane; MES, 4-morpholineethanesulfonic acid; HPLC, high pressure liquid chromatography; MS, mass spectrometry; DTT, dithiothreitol; PBS, phosphate-buffered saline.

RPE65 amino acid sequence, which reveal no predicted membrane spanning segments, including no N-terminal ER localization signal sequence. Proposed mechanisms of membrane binding include tethering via post-translational lipid modifications, electrostatic interactions with phospholipid head groups, and hydrophobic interactions between amino acid side chains and the hydrophobic core of the lipid bilayer. The recently determined crystal structure of RPE65 reveals that this enzyme is a single domain, amphiphilic protein containing a cluster of hydrophobic residues that surround the entrance of a tunnel leading to its catalytic center, which is defined by a bound iron cofactor. This arrangement suggests that portions of RPE65 integrate into the lipid bilayer and act as recognition elements to allow for the extraction of highly lipophilic retinyl ester substrates. This finding led us to hypothesize that the native membrane structure may be essential for the proper function of RPE65. Here, we present biochemical evidence supporting an indispensable role for the membrane phospholipid bilayer in RPE65 enzymatic activity.

EXPERIMENTAL PROCEDURES

Materials—Fresh bovine eyes were obtained from a local slaughterhouse (Mahan's Packing, Bristolville, OH). All-*trans*-retinol was prepared by reduction of all-*trans*-retinal with an excess of sodium borohydride in ethanol and then purified by preparative normal phase HPLC (Beckman Ultrasphere-Si; 5 μm; 10 $\times$ 250 mm) eluted with 10% ethyl acetate in hexane at a flow rate of 5 ml/min. Retinoid concentrations in ethanol were determined spectrophotometrically by using a molar absorbance coefficient of 52,770 M^{-1} cm^{-1} for all-*trans*-retinol. Phospholipases A_2 from honeybee venom or *Naja mossambica mossambica* as well as phospholipase C (PLC) from *Bacillus cereus* and phospholipase D (PLD) from *Streptomyces* sp. were purchased from Sigma. One unit of phospholipase A_2 enzymatic activity was defined as that which hydrolyzes 1.0 μmol of soybean phosphatidylcholine (PC) to L-α-lysophosphatidylcholine (lyso-PC) and a fatty acid per min at pH 8.9 and 25 °C.

Purification of RPE Microsomes—RPE microsomes were prepared from fresh bovine RPE by methods described previously (12). After ultracentrifugation, microsomes were resuspended in 10 mM BisTris propane buffer, pH 7.5, or 5 mM Tris-HCl, pH 7.0, containing 1 mM dithiothreitol (DTT). Total protein concentration was adjusted to 20 mg/ml measured by the Ultra-Bradford method (Novexin, Cambridge, UK). Aliquots of RPE microsomes (200 μl) were stored at −80 °C.

Extraction Procedures—Suspensions of RPE microsomes with protein concentrations of 20 mg/ml were diluted 1:10 into buffered solutions containing a variety of reagents described in the figures. With the exception of the pH titration experiments, solutions were buffered with 10 mM Tris-HCl, pH 7.0, and all contained 1 mM DTT. Mixtures were incubated on ice for 1 h prior to centrifugation except for those undergoing hydroxylamine, pH 7.0, treatment that was performed at 22 °C. Mixtures were centrifuged at 150,000 $\times$ *g* for 1 h to sediment insoluble material. Resulting pellets were resuspended in a volume of buffer equal to that of the recovered supernatant. Equal volumes of each fraction were analyzed by SDS-PAGE. The separated proteins were examined by Coomassie staining or immunoblotting.

Analysis of RPE Microsome Alkaline Extracts—RPE microsomes were suspended in a solution consisting of either 100 mM Na_2CO_3, pH 11.5, or 100 mM CAPS, pH 11.0, and 1 mM DTT, incubated on ice for 1 h, and then centrifuged at 150,000 $\times$ *g* for 1 h to sediment insoluble material. Supernatant fractions were collected and used for subsequent experiments. In one set of experiments, the pH of the extracts was adjusted to pH 6.0 by addition of MES, pH 6.0, to a final concentration of 50 mM followed by slow addition of a predetermined amount of 12.1 N HCl. After a 1-h incubation on ice, the samples were centrifuged at 150,000 $\times$ *g* for 1 h to sediment insoluble material. The supernatant was collected, and the pellet was resuspended in a volume of alkaline buffer equal to that of the supernatant. In the second set of experiments, 100 μl of alkaline extract was injected into a 20,000-kDa MWCO Slide-a-Lyzer dialysis cassette and dialyzed overnight against 1 liter of PBS containing 1 mM DTT at 4 °C. The retentate was removed from the cassette and centrifuged at 150,000 $\times$ *g* for 1 h to sediment insoluble material. The supernatant was collected, and the pellet was resuspended in a volume of PBS equal to that of the supernatant. In both experiments, the pH of the samples was tested to ensure that the desired value had been achieved. Equal volumes of each sample were analyzed by SDS-PAGE followed by Coomassie staining or immunoblotting.

Anapoe X-114 Phase Separation—Suspended RPE microsomes or the 20,000 $\times$ *g* supernatants obtained after centrifuging RPE homogenate at protein concentrations of ~1 mg/ml were incubated in a solution containing 10 mM Tris-HCl, pH 7.0, 150 mM NaCl, 1 mM DTT, and 1% w/v Anapoe X-114 (Anatrace) for 1 h on ice to allow solubilization of integral membrane proteins. Mixtures then were centrifuged at 150,000 $\times$ *g* for 1 h to sediment insoluble material. The resulting supernatant fractions were used for phase separation experiments. The phase separation procedure was performed essentially as described by Bordier (13) except that no precondensation of the detergent was performed because the detergent used in this study was purified by the manufacturer, and the last detergent rinse of the aqueous phase was omitted. Final aqueous and detergent-rich phases were equalized in volume by adding 10% w/v Anapoe X-114 and the solubilization buffer, respectively. Equal volumes of each fraction were analyzed by SDS-PAGE followed by Coomassie staining or immunoblotting.

LRAT and Retinoid Isomerization Assays—Reactions were carried out in mixtures of 10 mM BisTris propane buffer, pH 7.5, and 1% bovine serum albumin with 20 μl of bovine RPE microsomes. All-*trans*-retinol was delivered in 0.8 μl of *N,N*-dimethylformamide to a final concentration of 10 μM. Reactions were initiated by adding recombinant human apocellular retinaldehyde-binding protein (CRALBP) (20 μl of a 5 mg/ml stock solution) purified as described previously (14). The total volume of each reaction mixture was 200 μl. Unless otherwise indicated, reactions were incubated at 37 °C for 1 h and stopped by adding 300 μl of methanol followed by the same volume of hexane. Retinoids were extracted and analyzed by a Hewlett Packard 1100 series HPLC system (Agilent Technologies, Santa Clara,

CA) equipped with a diode array detector and a normal phase column (Beckman Ultrasphere-Si, 4.5 × 250 mm, 5 μm). Retinoids were separated by an isocratic flow of 10% ethyl acetate in hexane at 1.4 ml/min and detected at 325 nm. Two types of experiments were performed to test the effect of PLA_2 and different detergents on retinoid isomerization. In one set, PLA_2 or detergent was added to the reaction together with all-*trans*-retinol and CRALBP at time 0. Alternatively, RPE microsomes were preincubated with all-*trans*-retinol for 10 min at room temperature to ensure robust production of retinyl esters prior to adding CRALBP and the test component.

Generation and Epitope Mapping of Anti-RPE65 Monoclonal Antibody—Anti-RPE65 monoclonal antibody was raised against full-length recombinant human RPE65 protein expressed in Sf9 cells and purified as described in Golczak *et al*. (15). The purified protein was used to immunize mice as described previously (16). Purified RPE65 was emulsified with the adjuvant system (Sigma) according to the manufacturer's protocol, and the antigen (50 μg/body) was injected intraperitoneally into 4-week-old BALB/c mice. The same immunization procedure was repeated three times every 10 days. After immunization, mouse serum titers were checked by immunoblotting with purified RPE65 and bovine RPE microsomes. Purified native bovine RPE65 (30 μg/body) in PBS was used for the final immunization performed 48 h before the fusion. Hybridoma cell lines were prepared by fusion of SP2 mouse myeloma cells (American Type Culture Collection, Manassas, VA) (7.7×10^6) with splenocytes (2.3×10^7) from an immunized mouse by using polyethylene glycol 1500 (Roche Applied Science). Culture supernatants from the resulting hybridomas were screened with purified RPE65 and bovine RPE microsomes by enzyme-linked immunosorbent assay and immunoblotting. Positive hybridomas were subcloned three times by the method of limiting dilution in microtiter plates. IgG isotypes were examined with a mouse monoclonal isotyping test kit (Roche Applied Science). Five overlapping portions of RPE65 cDNA (GI:67188783), together encompassing the entire coding region, were amplified by PCR using PfuUltra high fidelity DNA polymerase (Stratagene, La Jolla, CA) and the following primers: (*a*) 5′-caccatgtctatccaggttgagcatcc-3′ and 5′-ctaggaaaatatattcttgcaggg-3′; (*b*) 5′-caccatggctttcccagatccctgc-3′ and 5′-ctaagtcagaccaaaactatgaacg-3′; (*c*) 5′-caccatgaagccatcttacgttcatag-3′ and 5′-ctacccattgtcttcatagg-3′; (*d*) 5′-caccatgttccatcacatcaacacc-3′ and 5′-ctatttcccacaatacttctgg-3′; and (*e*) 5′-caccatgtttgagtttcctcaaatcaattacc-3′ and 5′-ctaagatttttttgaacagtcc-3′. The resulting blunt-end PCR products were agarose gel-purified and cloned into the pET100/D-TOPO vector (Invitrogen) for protein expression in *Escherichia coli*. A second round of epitope mapping, using information from the first round, was performed to locate more precisely the epitope-containing region. The following PCR primers were used to amplify segments of the RPE65 cDNA that encode various portions of the C-terminal 115 amino acid residues where the epitope was located in the first round of mapping: 1) 5′-cacccctcaaatcaattaccagaagtattgtggg-3′ and 5′-agatttttttgaacagtccatggaaaggtgacaggg-3′; 2) 5′-caccggggtttggcttcatattgc-3′ and 5′-gccaagtccatacgcatatgtgtaagg-3′; 3) 5′-caccgggtttctgattgtggatctctgc-3′ and 5′-ccaagtttctttagttttgacattcagc-3′; 4) 5′-caccgggtttctgattgtggatctctgc-3′ and 5′-gctcaccaccacactcagaactacacc-3′; 5) 5′-caccgggtttctgattgtggatctctgc-3′ and 5′-ggcaacttcacttaagtccttggc-3′; and 6) 5′-caccgggtttctgattgtggatctctgc-3′ and 5′-ggcaacttcacttaagtccttggc-3′. The resulting blunt-end PCR products were agarose gel-purified and cloned into the pET102/D-TOPO vector for expression as thioredoxin fusion proteins (Invitrogen), and the accuracy of all constructs was confirmed by DNA sequencing. The resulting plasmids were used to transform Rosetta 2 (DE3)pLysS cells (Novagen, San Diego). Bacterial cultures grown in the presence of 50 μg/ml carbenicillin and 34 μg/ml chloramphenicol in LB media to an $A_{600\ nm}$ of 0.5 were induced with 1 mM isopropyl 1-thio-β-D-galactopyranoside for 4 h to allow expression of the fusion proteins. After 4 h, the cells were harvested by centrifugation and lysed with SDS-PAGE loading buffer. Proteins were separated by SDS-PAGE and analyzed by Coomassie staining and immunoblotting by using the anti-RPE65 monoclonal antibody described above.

Phospholipid Analysis—Synthetic and natural phospholipids purchased from Avanti Polar Lipids (Alabaster, AL) included 1,2-dioleoyl-*sn*-glycero-3-phosphocholine, 1,2-dioleoyl-*sn*-glycero-3-phosphoethanolamine, 1-palmitoyl-2-hydroxy-*sn*-glycero-3-phosphocholine, 1-palmitoyl-2-hydroxy-*sn*-glycero-3-phosphoethanolamine, chicken egg yolk phosphatidylcholine, and porcine brain phosphatidylethanolamine. RPE microsomal phospholipids were extracted by the Folch method (see Ref. 17). Thirty μl of RPE microsomes were diluted with 0.17 ml of 10 mM BisTris propane buffer, pH 7.4, and extracted with 0.3 ml of chloroform and 0.1 ml of methanol. The organic phase was collected and dried down in a SpeedVac. Main classes of extracted phospholipids were separated on an Agilent 1100 series HPLC system (Agilent Technologies). Phospholipids were redissolved in acetonitrile and injected onto a Zorbax RX-SIL column (Agilent Technologies) (2.1 × 150 mm, 5 μm). A linear gradient of methanol in acetonitrile (0–100%, 30 min, 1 ml/min) was used as the mobile eluting phase. The HPLC system was coupled to an LXQ high throughput linear ion trap mass spectrometer (Thermo Scientific, Waltham, MA) interfaced with an electrospray ionization source. Depending on the ionization mode, the mobile phase was supplemented with 0.1% formic acid (positive mode) or 10 mM ammonium formate (negative mode). The ion source and optic parameters were optimized for positive and negative modes with respect to the phospholipid standards. PC, PE, lyso-PC, and lyso-PE were quantified based on areas under peaks corresponding to the most abundant phospholipids detected in samples as follows: 1-palmitoyl-2-oleoyl-*sn*-glycero-3-phosphocholine, 1-palmitoyl-2-arachidonoyl-*sn*-glycero-3-phosphocholine, and 1-stearoyl-2-arachidonoyl-*sn*-glycero-3-phosphocholine for PC; 1-palmitoyl-2-arachidonoyl-*sn*-glycero-3-phosphoethanolamine, 1-stearoyl-2-arachidonoyl-*sn*-glycero-3-phosphoethanolamine, and 1-stearoyl-2-docosahexaenoyl-*sn*-glycero-3-phosphoethanolamine for PE; 1-palmitoyl-2-hydroxy-*sn*-glycero-3-phosphocholine and 1-stearoyl-2-hydroxy-*sn*-glycero-3-phosphocholine for lyso-PC; and 1-palmitoyl-2-hydroxy-*sn*-glycero-3-phosphoethanolamine and 1-stearoyl-2-hydroxy-*sn*-glycero-3-phosphoethanolamine for lyso-PE. Identification of phospholipids was based on their $(MS)^n$ fragmentation patterns. Total lipid content deter-

minations in RPE microsomes were based on inorganic phosphate concentrations according to the Baginski method (18). Phospholipids were submerged in 0.65 ml of 60% $HClO_4$ and hydrolyzed at 200 °C for 2 h. Then 3.4 ml of water followed by 0.5 ml of 2.5% ammonium heptamolybdate and 0.5 ml of 10% ascorbic acid was added to each sample. After 5 min of incubation at 100 °C, the absorbance at 797 nm was measured against water. The amount of inorganic phosphate was estimated from a standard calibration curve.

TABLE 1
Data collection and refinement statistics

Values in parentheses are for the highest resolution shell of data. $R_{sym}(I) = \Sigma_{hkl}\Sigma_i|I_i(hkl) - \langle I(hkl)\rangle|/\Sigma_{hkl}\Sigma_i I_i(hkl)$ with summation performed over all symmetry-equivalent reflections excluding those observed only once. r.m.s.d., root mean square deviation.

Data collection	
X-ray source	APS 23-ID-D
Temperature	100 K
Wavelength	1.03324 Å
Space group	$P6_5$
Unit cell constants	$a = b = 176.36$, $c = 86.72$ Å
Resolution	100 to 1.9 Å (1.97 to 1.90 Å)
Unique reflections observed	119,836
Completeness	99% (92%)
Multiplicity	4.7 (3.2)
$I/\sigma I$	17.5 (2.26)
$R_{sym}(I)$	10.4% (56.5%)
Average mosaicity	0.41°
Wilson *B* factor	23.2 Å^2
Chains per asymmetric unit	2
Solvent content	62%
Refinement	
Resolution range	20 to 1.9 Å (1.95 to 1.9 Å)
Unique reflections	113,526
Twin operator	$h + k, -k, -l$
Refined twin fraction	33.5%
Total refined atoms	8556
Protein	8051
Water	503
Iron	2
Average *B* factor	29 Å^2
Protein	28.7
Water	33.3
Iron	21.8
R_{work}	14.6% (21.2%)
R_{free}	17.1% (24%)
r.m.s.d. bond lengths	0.016 Å
r.m.s.d. bond angles	1.455°
Ramachandran plot	
Favored	97.9%
Outliers	0%

Cross-linking of Proteins Associated with RPE Microsomes—Isolated RPE65 microsomes from ~100 bovine eyes were washed twice with 67 mM phosphate buffer, pH 7.2, 150 mM NaCl (PBS) containing 1 mM EDTA, resuspended in 1 ml of the same buffer, and aliquoted into 50-μl samples prior to adding bis(maleimido)hexane (BMH) cross-linker (Pierce) up to 0.5 mM delivered in 0.5 μl of *N,N*-dimethylformamide. The cross-linking reaction was carried out at room temperature for 15 min. Samples then were quenched with 2 mM β-mercaptoethanol and analyzed by SDS-PAGE and immunoblots with either commercially available RPE65 antibodies (Novus Biologicals, Littleton, CO) or anti-LRAT antibodies described elsewhere (19).

Purification of Cross-linked Products and Identification of Proteins Associated with RPE65—After incubation of RPE microsomes with BMH, the cross-link reaction was stopped with β-mercaptoethanol as described above. RPE microsomes were washed twice with 6 ml of PBS and solubilized in 2 ml of 40 mM CHAPS in PBS. After 1 h of incubation at 4 °C, unsolubilized material was pelleted by centrifugation at 130,000 × *g* for 1 h at 4 °C. The supernatant was diluted four times with PBS and loaded onto 0.5 ml of CNBr-activated agarose resin coupled to anti-RPE65 monoclonal antibodies according to the manufacturer's protocol and equilibrated with 10 mM CHAPS in PBS. The loading procedure was repeated twice at a flow rate of 0.5 ml/min to ensure high binding efficiency. The resin then was washed with 10 ml of loading buffer. Bound proteins were eluted with 0.1 M glycine HCl, pH 2.3. Fractions containing eluted proteins were analyzed by SDS-PAGE and immunoblotting developed against RPE65. Distinct protein bands were cut out from gels, digested with trypsin according to a published protocol (20), and analyzed by mass spectrometry at the Center for Proteomics and Bioinformatics at Case Western Reserve University. Alternatively, fractions containing purified RPE65 and its cross-linked complexes were pooled together, and the proteins were precipitated by a chloroform/methanol procedure (21). Protein pellets were resuspended in 5 μl of 50% formic acid in water; the acid was neutralized with 0.2 ml of 200 mM ammonium bicarbonate, and the proteins were digested with sequence grade trypsin overnight at 37 °C. Peptides were loaded onto a C18 reverse phase column and separated in a linear gradient of aceto-

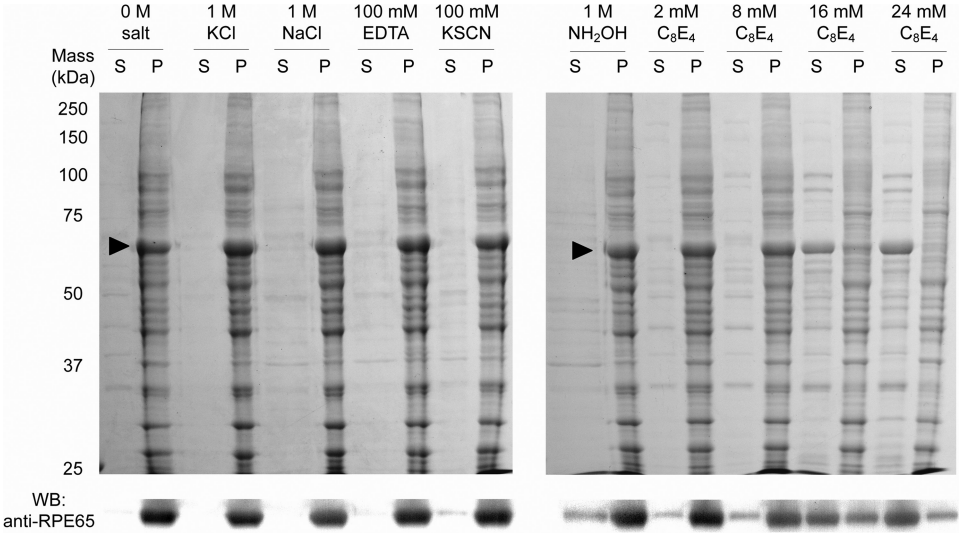

FIGURE 1. **SDS-PAGE analysis of bovine RPE microsomal proteins after incubation with reagents known to solubilize certain classes of membrane proteins.** Supernatant (*S*) and pellet (*P*) fractions obtained after incubating microsomes with the indicated compounds for 1 h on ice followed by centrifugation at 150,000 × *g* for 1 h were separated by SDS-PAGE, and the resulting gels were either stained with Coomassie Brilliant Blue (*upper panels*) or used for immunoblotting with an anti-RPE65 antibody (*lower panels*). The results clearly show that only C_8E_4 treatment at concentrations above the CMC resulted in significant extraction of RPE65. The *arrowhead* indicates the position of RPE65. *WB*, Western blot.

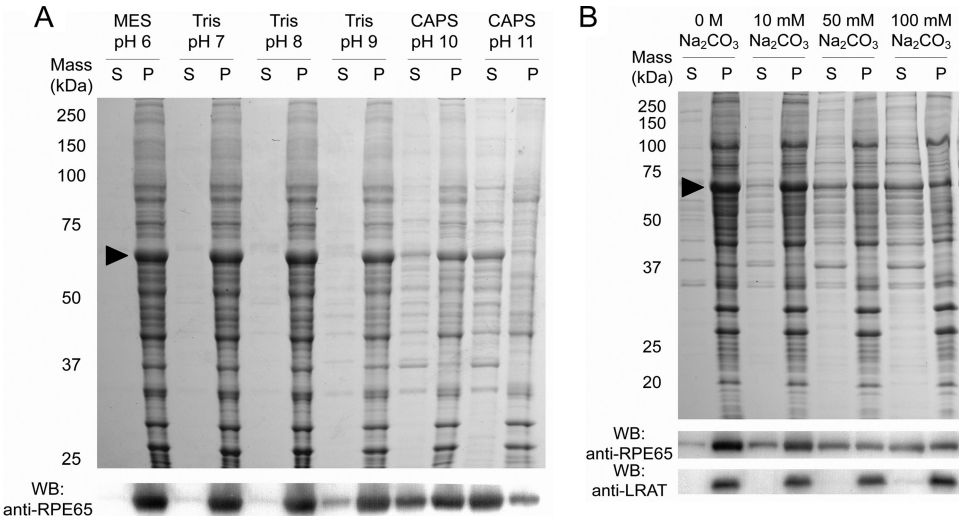

FIGURE 2. **Effects of pH and buffer concentration on the distribution of RPE65 in microsomal supernatant and pellet fractions.** Supernatant (*S*) and pellet (*P*) fractions obtained after incubating microsomes with the indicated compounds for 1 h on ice followed by centrifugation at 150,000 × *g* for 1 h were separated by SDS-PAGE, and the resulting gels were either stained with Coomassie Brilliant Blue (*upper panels*) or used for immunoblotting with anti-RPE65 and anti-LRAT antibodies (*lower panels*). *A,* significant extraction of RPE65 occurred when microsomes were incubated with 50 mM CAPS, pH 11.0, but not at lower pH values. The final concentration of buffers in this experiment was 50 mM. *B,* RPE65 extraction increased after incubation with higher concentrations of Na_2CO_3. After incubation in 100 mM Na_2CO_3, pH 11.5, ~50% of the RPE65 was extracted from the microsomes. The *arrowhead* indicates the position of RPE65. *WB*, Western blot.

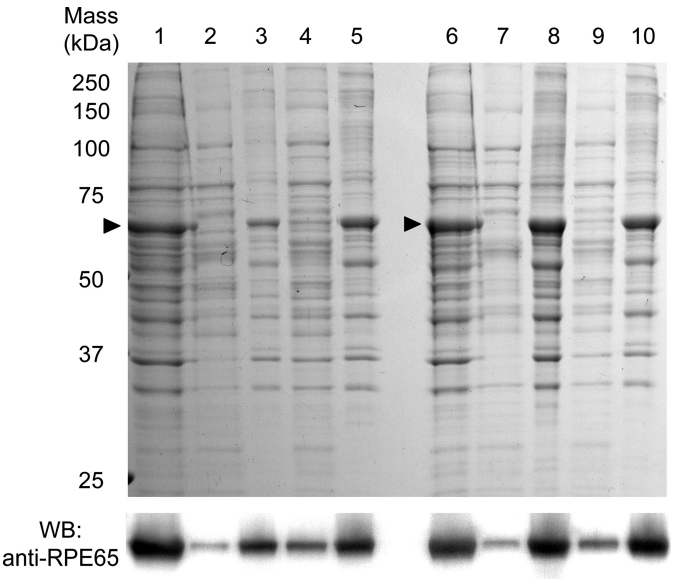

FIGURE 3. **Behavior of RPE microsomal alkaline extracts after pH neutralization or dialysis.** RPE microsomes were treated with either 100 mM Na_2CO_3, pH 11.5, or 100 mM CAPS, pH 11.0, for 1 h on ice and then centrifuged for 1 h at 150,000 × *g*. The supernatant fractions after Na_2CO_3 and CAPS treatment are shown in *lanes 1* and *6*, respectively. After adjusting the pH of these extracts to six and incubating them on ice for 1 h, samples were centrifuged at 150,000 × *g* for 1 h to determine whether RPE65 remained in the supernatant. The supernatant and pellet fractions from this experiment for the pH-adjusted Na_2CO_3 and CAPS extracts are shown in *lanes 2* and *3* and *lanes 7* and *8*, respectively. Alternatively, we dialyzed the alkaline extracts overnight at 4 °C against PBS containing 1 mM DTT. Afterward, the retentates were collected and centrifuged at 150,000 × *g* for 1 h to assess the solubility of RPE65 after removal of the extraction agent and adjustment of pH to 7.4. The supernatant and pellet fractions from this experiment with Na_2CO_3 and CAPS extracts are shown in *lanes 4* and *5* and *lanes 9* and *10*, respectively. In both experiments RPE65 became insoluble upon return to more physiological pH values. The *arrowhead* indicates the position of RPE65. *WB*, Western blot.

nitrile in water (2–100% in 45 min). The eluent was injected into an LTQ-FT ultra mass spectrometer (Thermo Scientific). MS data were analyzed with the aid of Mascot Deamon software version 2.2.0 (Matrix Science Ltd., Boston) and the Massmatrix data base search engine (22, 23).

Crystallographic Analysis of RPE65—Bovine RPE65 from native RPE membranes was purified as described previously (24). Purified protein at a concentration of 15 mg/ml was crystallized by the hanging drop vapor diffusion method by mixing 1 μl each of protein solution and a crystallization solution consisting of 100 mM MES, pH 6.0, 30% v/v polyethylene glycol 200, and 2 mM DTT at room temperature and incubating the resulting drops over 0.5 ml of the crystallization solution at 8 °C. Crystals appeared within a day and grew to final size within a few weeks. Crystals were harvested in Hampton loops (Hampton Research, Aliso Viejo, CA) and flash-cooled in liquid nitrogen prior to x-ray exposure. A 1.9-Å resolution dataset was collected at the APS 23-ID-D beamline. Data were reduced by using HKL2000 (25) and TRUNCATE (26). Analysis of the data with phenix.xtriage from the PHENIX suite (27) revealed that the crystal was merohedrally twinned. As the crystal was found to be isomorphous to those described previously (24), direct refinement of the existing model (PDB accession code 3FSN) against the higher resolution dataset was performed with REFMAC5 (28). Reflections used for cross-validation in the lower resolution dataset were maintained as free reflections in the current dataset. The amplitude-based twin refinement option in REFMAC5 was used to account for the significant (33.5%) merohedral twinning in the crystal. Several cycles of REFMAC5 refinement followed by manual rebuilding with the program Coot (29) resulted in a final R_{free} value of 17.1% with good stereochemistry as assessed by MolProbity (30). It should be noted that the somewhat lower than expected *R* values are a consequence of the altered statistical properties associated with twinned crystals. Residues 1, 2, 108–126, 198–200, and 261–272 were omitted from the final model because of weak electron density. The model and structure factor amplitudes have been deposited with the Protein Data Bank under accession code 3KVC. Data collection and refinement statistics are shown in Table 1.

RESULTS

Extraction and Phase Separation Experiments—To determine the predominant type of interaction responsible for binding of RPE65 to native RPE microsomal membranes, we exposed microsomes to a variety of treatments known to solubilize peripheral or integral membrane proteins. As shown in

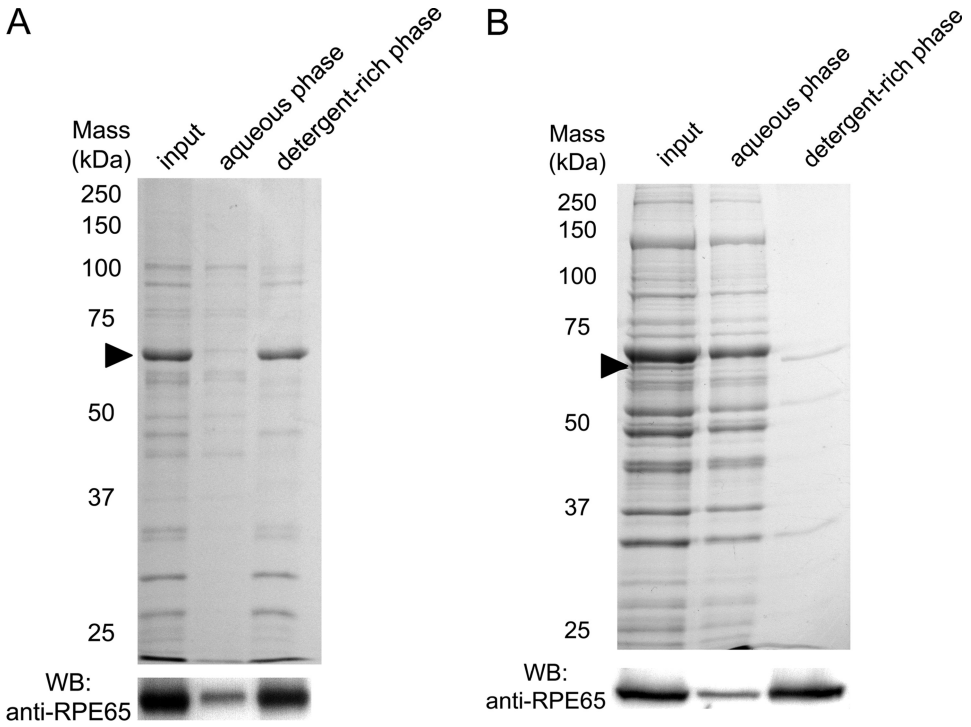

FIGURE 4. **Partitioning of RPE65 in Anapoe X-114 phase separation experiments.** RPE65 microsomes (*A*) or the 20,000 × *g* supernatant (*B*) obtained after centrifugation of homogenized bovine RPE were solubilized in 1% w/v Anapoe X-114 (Anatrace), and mixtures were centrifuged at 150,000 × *g* for 1 h to sediment insoluble material. Supernatant fractions obtained after centrifugation were used for the phase separation studies performed as described under "Experimental Procedures." *Input* indicates total proteins found in the supernatant fractions after high speed centrifugation; *aqueous phase* indicates proteins remaining in the detergent-poor top phase after phase separation, and *detergent rich-phase* indicates the proteins found in the small oily droplet at the bottom of the sucrose cushion after phase separation and low speed centrifugation. RPE65 strongly partitioned into the detergent-rich phase in both experiments, demonstrating its amphiphilic nature. The *arrowhead* indicates the position of RPE65. *WB*, Western blot.

Fig. 1, virtually no RPE65 was extracted when microsomes were exposed to solutions containing low or high salt concentrations, the chaotropic agent KSCN, or the divalent cation chelating agent EDTA. Furthermore, treatment with a high concentration of hydroxylamine, which cleaves thioester bonds, did not extract significant amounts of RPE65. These data suggest that binding of RPE65 to native membranes is not dominated by electrostatic interactions or by palmitoyl anchoring. However, as we have observed and as recently reported in the literature (31), exposure of microsomes to strong alkaline conditions results in the extraction of significant amounts of RPE65 (Fig. 2, *A* and *B*). It was hypothesized that exposing basic residues on the surface of RPE65 to increasing pH would liberate the protein by disrupting its electrostatic interactions with membrane phospholipid head groups. If this hypothesis is correct and RPE65 is a true peripheral membrane protein, it should remain soluble after lowering the pH back to a more physiological value or removing the solubilizing agent (32, 33). Alternatively, the apparently soluble RPE65 could be generated by denaturation of the protein in strong alkaline conditions or by formation of nonsedimentable lipoprotein particles, which is well known to occur in alkaline conditions (33). To test these hypotheses, we adjusted the pH of Na_2CO_3 or CAPS alkaline microsomal extracts to pH 6.0 and, after 1 h of incubation on ice, centrifuged the sample at 150,000 × *g* for 1 h to sediment particulate matter. In a separate experiment, we dialyzed these alkaline extracts overnight against PBS containing 1 mM DTT to remove the solubilizing agent and return the pH to 7.4. As shown in Fig. 3, most of the RPE65 became insoluble after either treatment suggesting that alkaline-extracted RPE65 was either denatured or not in true solution. The behavior of RPE65 in this experiment further argues against a peripheral association of the protein with the native membrane. Detergent, especially the nonionic detergent C_8E_4 at concentrations above its CMC, is the most effective agent for extracting RPE65 (Fig. 1), and the resulting solubilized protein is highly stable. The structural integrity of this detergent-solubilized protein is supported by its successful and robust crystallization (24). The last finding suggests that the interaction of RPE65 with native membranes is predominantly hydrophobic. To further demonstrate that hydrophobic rather than electrostatic forces dominate the RPE65-membrane interaction, we performed Anapoe X-114 phase separation experiments using a well established procedure (13). Here, water-soluble and peripheral membrane proteins can be separated from integral membrane proteins based on the selective partitioning of integral proteins into a detergent-rich phase that develops after raising the temperature of the solution. We performed this experiment using the Anapoe X-114-solubilized RPE microsomes, where RPE65 is the single most abundant protein, as well as the 20,000 × *g* supernatant fraction obtained after centrifugation of homogenized bovine RPE, where RPE65 makes up a small fraction of total protein. Consistent with previous reports (34, 35), we found in both experiments that RPE65 resided predominantly in the detergent-rich phase thus demonstrating the integral membrane behavior of the protein in this assay (Fig. 4, *A* and *B*). Because Anapoe X-114 is a nonionic detergent, the interaction of RPE65 with the detergent micelle must be attributed to hydrophobic rather than electrostatic forces.

Effect of PLA_2 on Retinoid Isomerization Activity in RPE Microsomes—RPE65 is susceptible to rapid loss of its enzymatic activity upon exposure to a variety of detergents even at concentrations below their CMC values (36, 37). To elucidate the putative role of phospholipids in *trans*-to-*cis*-retinoid isomerization, we exposed bovine RPE microsomes to PLA_2 enzymatic activity. This lipase preferentially cleaves PC and PE to their corresponding lysophospholipids. Because hydrolysis occurs at the *sn*-2 position of phospholipids, a relatively mild perturbation of the lipid bilayer results as compared with that following

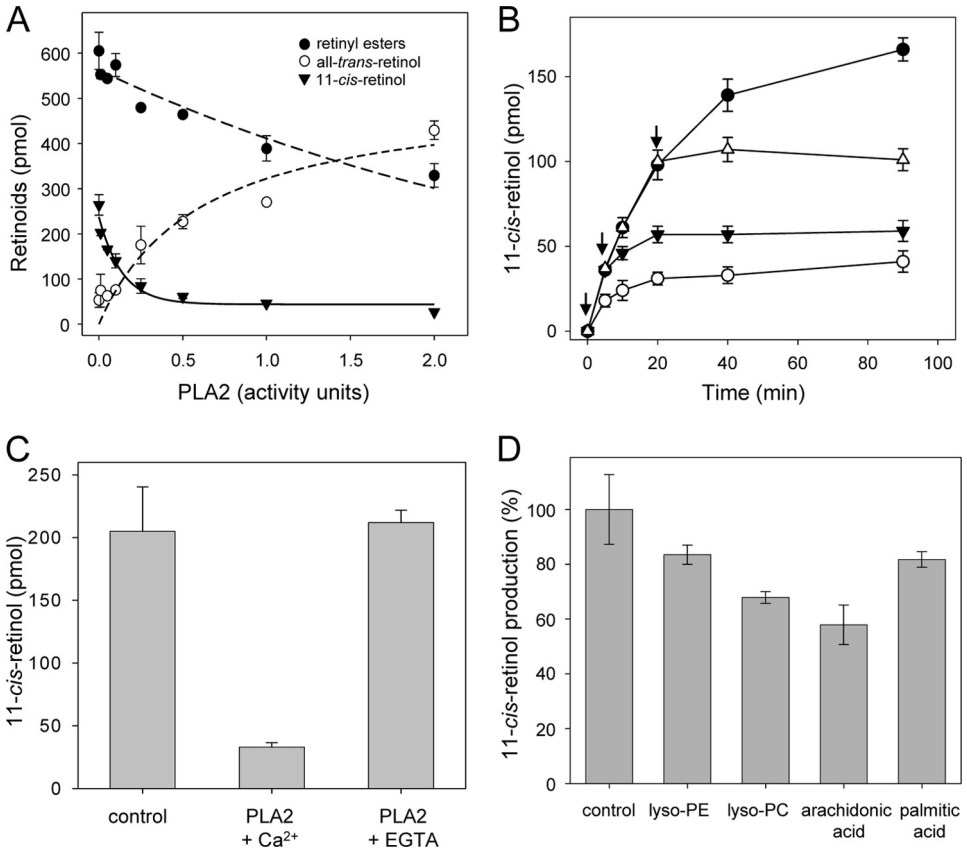

FIGURE 5. **Effects of PLA_2 treatment or the products of PLA_2 enzymatic activity on retinoid isomerization by bovine RPE microsomes.** *A,* retinoid isomerization reaction was performed in the presence of 0.5 mM $CaCl_2$, and 10 μM of all-*trans*-retinol was used as the substrate for retinyl ester formation. Increasing amounts of PLA_2 were added to the reaction mixture just prior to incubation at 37 °C. Low levels of PLA_2 activity markedly inhibited 11-*cis*-retinol production, whereas higher levels depleted the retinyl ester pool with a concomitant increase in all-*trans*-retinol production. *Error bars* were calculated from three independent experiments performed in duplicate. *B,* addition of PLA_2 (0.5 activity units) to an ongoing isomerization reaction rapidly inhibited further production of 11-*cis*-retinoids. *Arrows* indicate time points at which PLA_2 was added to the assay mixture. *Open circles, closed triangles,* and *open triangles* indicate reactions in which PLA_2 was added at 0, 5, and 20 min, respectively. *Closed circles* represent an untreated reaction. The inhibitory effect cannot be explained by competition between LRAT and PLA_2 for a common substrate (PC) because retinyl esters were rapidly synthesized at an early stage of this reaction. Thus, the supply of substrate for RPE65 was not affected by PLA_2 activity. *C,* inhibition of 11-*cis*-retinol formation by PLA_2 was Ca^{2+}-dependent. Assays were performed in the presence of 0.5 mM $CaCl_2$ or 1 mM EGTA to chelate residual Ca^{2+} ions. This experiment indicates that the inhibitory effect of PLA_2 is attributable to its calcium-dependent enzymatic activity toward phospholipids. *D,* excess of lyso-PE, lyso-PC, arachidonic, or palmitic acid (300 μM) was preincubated with RPE microsomes for 5 min at room temperature prior to addition of all-*trans*-retinol and CRALBP. Levels of 11-*cis*-retinol produced indicate that the striking effect of PLA_2 cannot be totally explained by direct inhibition caused by products of its enzymatic activity because concentrations of lysophospholipids or carboxylic acids corresponding to those in the total membrane digest only modestly slowed the reaction.

treatment with detergents. Incubation with increasing amounts of PLA_2 strongly inhibited 11-*cis*-retinol production from endogenous all-*trans*-retinyl palmitate in RPE microsomes (Fig. 5*A*). Although PLA_2 treatment resulted in a gradual decrease in retinyl ester content, far lower concentrations of PLA_2 caused a rapid loss of 11-*cis*-retinol production without substantially reducing the pool of available retinyl esters (<20%). PC is a substrate for both PLA_2 and LRAT. To ensure that the observed effect of PLA_2 in inhibiting 11-*cis*-retinol production was not caused by competition for the lipid substrate between these two enzymes, RPE microsomes were preincubated with all-*trans*-retinol to provide robust retinyl ester biosynthesis prior to addition of PLA_2. The resulting excess of retinyl esters synthesized *in situ* did not prevent rapid loss of 11-*cis*-retinoid production in PLA_2-treated membranes. Thus, the observed effect of PLA_2 on 11-*cis*-retinol production cannot be simply attributed to depletion of retinoid substrate due to the limited availability of PC for retinyl ester formation. A similar conclusion can be drawn from an experiment in which PLA_2 was added to an ongoing isomerization reaction that resulted in rapid inhibition of 11-*cis*-retinol production (Fig. 5*B*). The effect of PLA_2 was ablated by addition of EGTA, strongly suggesting that inhibition of retinoid isomerization directly relates to the calcium-dependent enzymatic activity of PLA_2 (Fig. 5*C*). Comparable results were obtained upon treatment of RPE microsomes with phospholipases class C and D (data not shown). To investigate whether inhibition of the isomerization reaction is caused by products of phospholipid hydrolysis, we performed the isomerization reaction in the presence of lyso-PC, lyso-PE, arachidonic acid, and palmitic acid. We first determined the total amount of phospholipids in the RPE microsomal fraction used for the isomerization assay to be 0.15 μmol. To test the most extreme condition, wherein all phospholipids become hydrolyzed, the same amount of lyso-PC, lyso-PE, arachidonic acid, and palmitic acid was added to the isomerization assay. Despite an excess of these compounds, only relatively modest decreases in 11-*cis*-retinol production occurred, possibly due to the detergent properties of these compounds (Fig. 5*D*). Thus, inhibition of retinoid isomerization upon PLA_2 treatment is not caused by the presence of products of phospholipid hydrolysis. Interestingly, prolonged treatment of RPE microsomes with PLA_2 led to elevation of all-*trans*-retinol levels in the examined samples (Fig. 5*A* and Fig. 6*A*). Because PLA_2 itself lacks esterase activity toward retinyl esters (data not shown), it is possible that phospholipid hydrolysis leads to a more relaxed membrane structure than that present in native membranes. This in turn might enhance substrate accessibility to retinyl esterases. To determine whether accumulation of all-*trans*-retinol itself affects retinoid isomerization, the assay was performed in the presence of increasing concentrations of all-*trans*-retinol. Despite robust LRAT activity, addition of excess retinol caused only

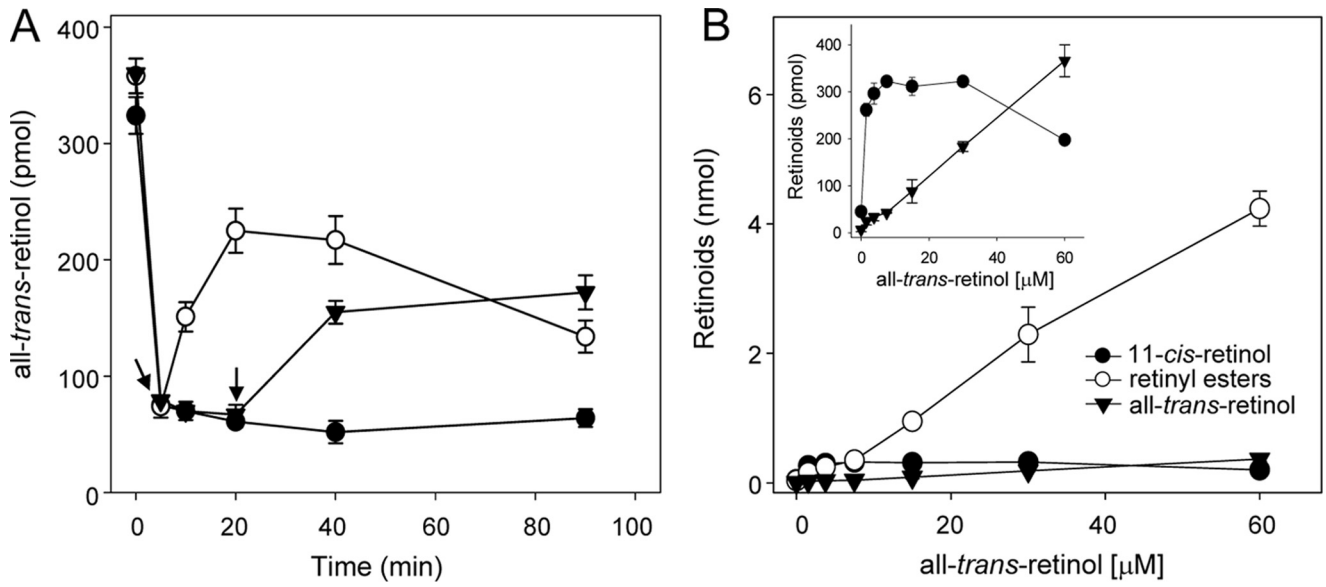

FIGURE 6. **Retinoid isomerization is not inhibited by an excess of all-*trans*-retinol.** *A,* concomitantly with modification of the phospholipid environment upon PLA_2 addition, increasing levels of all-*trans*-retinol were observed. *Arrows* indicate time points at which 0.5 unit of PLA_2 was added to the assays. *Open circles* and *closed inverted triangles* correspond to reactions in which PLA_2 was added at 5 and 20 min, respectively. *Closed circles* represent an untreated reaction. The initial precipitous drop in all-*trans*-retinol was caused by rapid esterification by LRAT. *B,* dose-dependent effect of all-*trans*-retinol on formation of the 11-*cis* isomer reveals that elevated retinoid levels had only a modest influence on the isomerization reaction. *Curves* in the *inset* are identical to those in the main figure but placed on a different scale that clearly shows a linear increase in free all-*trans*-retinol with increasing concentrations of added all-*trans*-retinol.

a gradual increase in "free" all-*trans*-retinol without affecting 11-*cis* isomer production (Fig. 6*B*).

Loss of Isomerization Activity after PLA_2 Treatment Correlates with Depletion of PC and PE in RPE Microsomes—Because the decrease in isomerization activity after PLA_2 treatment cannot be explained by a diminished concentration of membrane-dissolved retinyl esters or by product inhibition, we tested whether progressive loss of intact phospholipids *per se* correlates with the loss of 11-*cis*-retinol production. Standard retinoid isomerization reaction mixtures were incubated with PLA_2 for 20 min and then divided into 2 aliquots. One was treated with hexane to analyze retinoid composition, and the other was extracted with chloroform to determine lipid composition. As expected, liquid chromatography-mass spectrometry analysis of phospholipid content revealed a PLA_2-dependent progressive decrease in PC and PE accompanied by appearance of their corresponding lysophospholipids (Fig. 7*A*). Importantly, these changes in phospholipid composition directly correlated with the decline in 11-*cis*-retinol biosynthesis (Fig. 7*B*). Loss of 50% of the isomerization activity was observed when ~10% of PC and 40% of PE were hydrolyzed to their lyso-products. Accumulation of lysophospholipids and arachidonic acid resulting from PLA_2 enzymatic activity has been shown to change membrane morphology and electrostatics (38, 39). Therefore, RPE65 isomerization activity appears to be affected by modifications in membrane structure with increased fluidity.

To further investigate the effect of membrane fluidity, we assessed retinoid isomerization in the presence of cholesterol. By filling in spaces between phospholipids in the membrane bilayer, cholesterol increases its mechanical rigidity and lateral organization (40). Thus, in contrast to membrane destabilization caused by PLA_2 treatment, enrichment of RPE microsomes with cholesterol should preserve retinoid isomerization activity. Our experimental data fully support this hypothesis because incubation of RPE microsomes with cholesterol (independent of the delivery method) did not alter 11-*cis*-retinol production.

Modification of Phospholipid Membrane Structure Causes Rearranged Protein Composition in RPE Microsomes—Changes in phospholipid composition may have a profound impact on membrane-associated proteins by affecting their enzymatic activities (41–43). One of the outcomes resulting from relaxation of membrane structures caused by loss of intact phospholipids and lysophospholipid accumulation is dissociation of membrane protein components. Indeed, treatment of RPE microsomes with PLA_2 released a pool of membrane-associated proteins, including LRAT, but failed to liberate RPE65 (Fig. 8*A*). The detached LRAT remained active as determined with diheptanoyl-PC used as a lipid substrate (data not shown). A destabilized lipid bilayer may also affect the organization of membrane proteins by influencing their physical interactions with each other (44, 45). RPE65 was efficiently chemically cross-linked with other protein components in native RPE microsomes (Fig. 8*B*, *left panel*). Notably, PLA_2-dependent hydrolysis of phospholipids abolished formation of this RPE65 complex (Fig. 8*C*). Moreover, the dimeric form of LRAT was observed in the same experiment, indicating that, as with RPE65, PLA_2 treatment perturbed LRAT organization in membranes inducing its oligomerization (Fig. 8*C*) (46). Although the function of the RPE65 complex in retinoid isomerization remains to be established, its sensitivity to PLA_2 treatment implies an important role in maintaining membrane composition and structure for effective retinoid metabolism.

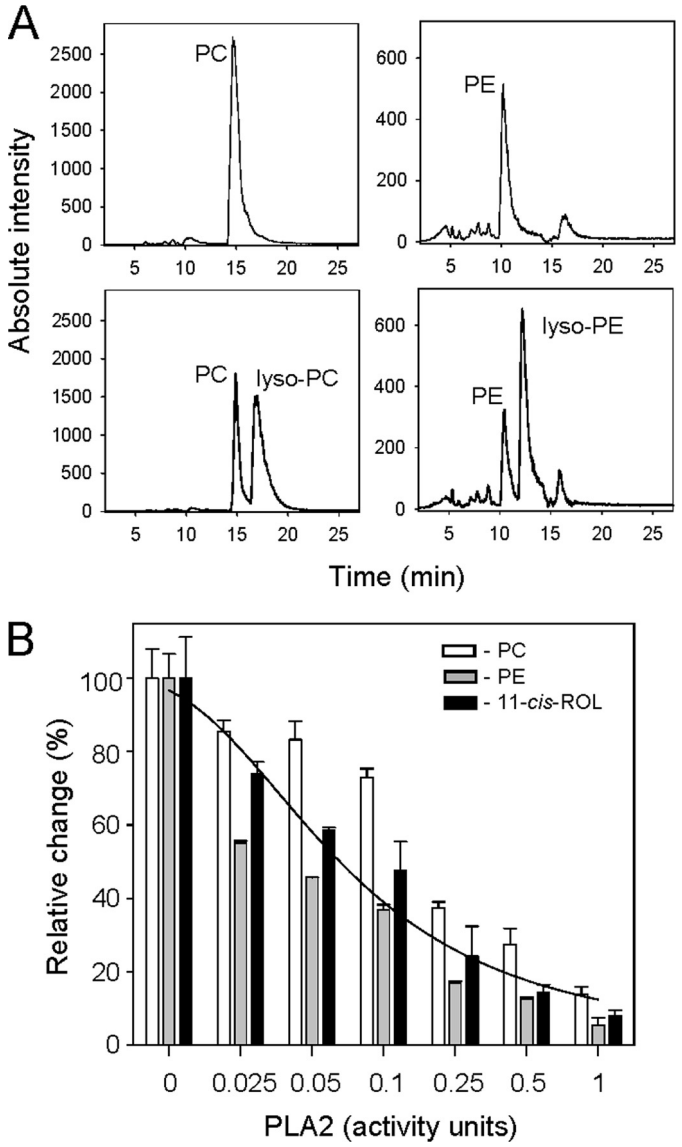

FIGURE 7. **Correlation between phospholipid hydrolysis and loss of 11-*cis*-retinol production.** *A,* liquid chromatography-mass spectrometry analysis of PC and PE content in RPE microsomes before (*top panels*) and after (*bottom panels*) treatment with 0.05 unit of PLA_2. Panels show extracted ion chromatograms at *m/z* 760, 782 for PC; 762, 740 for PE; 518, 496 for lyso-PC, and 454, 476 for lyso-PE. These correspond to the most intense peaks found for the named class of phospholipids. Amounts of phospholipids detected in each sample were estimated based on the area below the peaks and compared with standard curves prepared from synthetic standards at their linear dynamic range between 0.1 and 5 μmol. *B,* quantification of changes in 11-*cis*-retinol and phospholipid levels after PLA_2 treatment. Progressive hydrolysis of PC and PE correlates with gradual loss of RPE65 activity manifested by decreased 11-*cis*-retinol formation. The trend line follows a decline in 11-*cis*-retinol production.

Purification and Characterization of the Cross-linked RPE65 Complex—The homobifunctional cross-linking reagent BMH reacts specifically with sulfhydryl groups of cysteine side chains. Therefore, this compound can potentially covalently link two different polypeptide chains in close proximity (~13 Å from one another) permitting instrumental identification of proteins forming complexes in native tissues. To simplify analysis, the cross-linked RPE65 complex was purified on antibody affinity resin prior to MS study, and a monoclonal antibody directed against RPE65 was generated and characterized for this purpose. To map the region of protein recognized by the antibody, we first subdivided the sequence of RPE65 into five fragments that were expressed as N-terminal His_6 fusion proteins in *E. coli*. This initial screen localized the epitope to a C-terminal region of the protein consisting of residues 419–533. To more precisely locate the epitope, constructs were created that code for progressively longer portions of the RPE65 C terminus (Fig. 9*A*). The fragments were expressed as thioredoxin fusion proteins at high levels in *E. coli* (Fig. 9*B*, *left*). Immunoreactivity against fragments 5 and 6 indicate that the epitope is located within or immediately surrounding residues 492–514 (Fig. 9*B*, *right*). This region contains surface-exposed loops and a β-strand suggesting that this antibody could be used to recognize natively folded RPE65. Indeed, the biochemical properties of this antibody made it suitable for affinity purification of native RPE65 in the presence of detergents, including CHAPS and C_8E_4.

The first step of analysis required identification of proteins associated with RPE65. For this purpose, the Coomassie-stained band corresponding to isolated cross-linked RPE65 complex was cut out from an SDS-polyacrylamide gel and in-gel digested with trypsin (Fig. 10*A*). Peptides found in the extracted gel revealed almost exclusively the presence of retinol dehydrogenase 5 (RDH5) and retinal G protein-coupled receptor (RGR) accompanied by RPE65 and common contaminants like keratin, consistent with the 30–40-kDa increase in the molecular mass observed in SDS-polyacrylamide gels (Fig. 10*A*; Table 2). In the second stage and knowing the sequences of the RPE65-associated proteins, we used the Massmatrix data base search engine to automatically analyze and identify all possible combinations of tryptic peptides from RPE65, RDH5, and RGR linked via a cysteine residue in a series of proteolytic digests. Candidate ions were further verified by comparison of predicted and experimental MS/MS spectra. From an extensive analysis of all these ions, we were able to identify with sufficient confidence only one pair of cross-linked peptides corresponding to RPE65 and RDH5. Based on the experimental data, Cys-175 within the RDH5 peptide ^{167}LAANGGGYCVSK^{178} and Cys-231 within the RPE65 sequence ^{223}SEIVVQFPCSDR^{234} become cross-linked and so are likely to be in close vicinity to each other in native RPE membranes (Fig. 10, *B* and *C*). Unfortunately, despite best our efforts, we were unable to map the putative interaction site between RPE65 and RGR.

Analysis of the Improved Resolution RPE65 Diffraction Data Set—In screening for crystals with an improved diffraction compared with our previously published dataset (24), we obtained a crystal that diffracted x-rays to a maximal resolution of 1.9 Å, a significant improvement over the 2.14 Å resolution dataset previously reported (Table 1). This crystal happened to be significantly merohedrally twinned. However, by including a twin target in the refinement procedure, as implemented in REFMAC5 (28), we obtained a high quality model with good crystallographic statistics. One of our goals was to acquire an electron density map that would allow modeling of the segment (residues 109–126) of the RPE65 chain that was missing in the previously reported model. But despite the improved overall resolution of the data, we observed that segments of the protein thought to be involved in membrane binding were even more

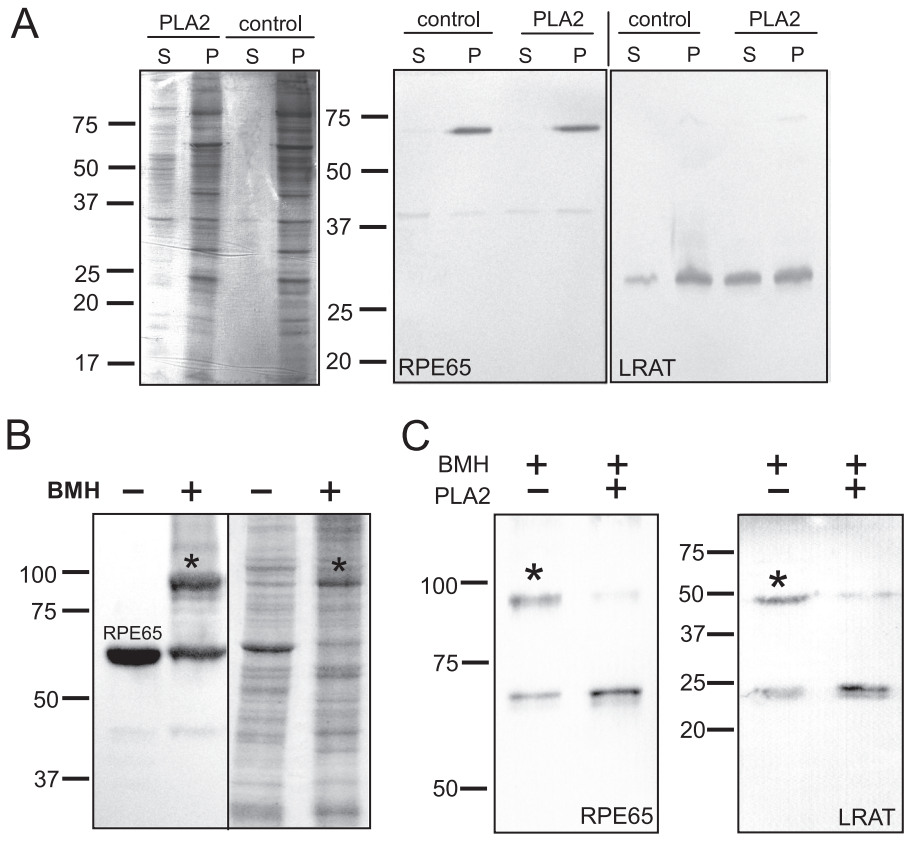

FIGURE 8. **Modification of phospholipid environment influences protein-protein interactions in RPE microsomes.** *A,* RPE microsomes were treated with 0.5 unit of PLA_2 in BisTris propane buffer, pH 7.4, and 0.5 mM $CaCl_2$ for 20 min at room temperature. After the sample was ultracentrifuged at 130,000 × *g* for 1 h at 4 °C, proteins in the collected pellet (*P*) and supernatant (*S*) fractions were separated by SDS-PAGE and analyzed by both Coomassie staining (*left panel*) and immunoblotting (*right panels*). Changes in phospholipid composition resulting from PLA_2 treatment led to dissociation of membrane-associated proteins (*left panel*). The pool of released proteins included the bitopic membrane protein LRAT but not RPE65 (*right panels*). *B,* detection of a cross-linked RPE65-containing complex in native RPE microsomes. *Asterisks* indicate migration of RPE65 and its BMH cross-linked form in 12% acrylamide gels as detected by immunoblot (*left panel*) and SDS-PAGE (*right panel*). *C,* hydrolysis of phospholipids by PLA_2 destabilized the RPE65 complex, so it was not trapped by chemical cross-linking (*left panel*). Formation of an LRAT dimer detected under similar conditions appears to be affected by changes in the phospholipid environment as well (*right panel*). *Asterisks* indicate positions of the cross-linked RPE65-containing complex or LRAT dimer.

highly disordered in this crystal such that residues 108–126, 198–200, and 261–272 had to be omitted from the final model. In general, the structure was highly similar to the one previously reported. As before, we observed two regions containing residual electron density in the active site of the enzyme. Their shapes were essentially identical to those previously observed. Notably, we now can identify water molecules bound in the inner cavity of the protein that may be catalytically relevant.

DISCUSSION

Even before the identification of RPE65 as the visual cycle retinoid isomerase, the membrane-bound nature of the retinoid isomerization activity in the RPE was appreciated. Bernstein *et al.* (47, 48) first reported that retinoid isomerization activity was associated with microsomal fractions from the RPE and that this activity was rapidly lost upon addition of a variety of detergents. Cloning of RPE65 in 1993 by two groups demonstrated that the RPE65 sequence lacks features that are typically associated with integral microsomal membrane proteins such as an N-terminal signal sequence and potential transmembrane segments (49, 50).

Although detergent was known to optimally solubilize RPE65, it was reported that a significant amount of RPE65 could be extracted from microsomes during incubation with 1 M KCl. This led to the conclusion that RPE65 is a peripheral rather than an integral membrane protein (34). The assertion that 1 M KCl can strip nearly all RPE65 from microsomes is what led to the incorrect conclusion that RPE65 is not "the" visual cycle retinoid isomerase (51). Later reports indicated that RPE65 exists in soluble and membrane-bound forms and that the post-translational addition of palmitoyl groups conferred microsomal membrane affinity (52–54). Recently, a report suggested that RPE65 membrane affinity is primarily a result of electrostatic interactions between RPE65 and phospholipid headgroups (31).

In re-examining the interaction of RPE65 with native microsomal membranes and in contrast to previous reports, we failed to observe significant solubilization of RPE65 upon incubation of resuspended microsomes in solutions containing 1 M KCl or 1 M NaCl. This observation provides strong evidence that the interaction of RPE65 with phospholipid membranes is not purely electrostatic in nature. Moreover, it also explains why high salt treatment of RPE microsomes did not reduce the membrane-bound retinoid isomerization activity as reported previously (51). Strong alkaline conditions have recently been shown to extract significant amounts of RPE65 from microsomes (31). We confirmed this effect but also found that either adjustment of the extract pH to 6.0 or dialysis of the extract against PBS to remove the extraction agent converted RPE65 to a particulate form that sedimented upon centrifugation. The last result suggests that the apparently solubilized RPE65 was either denatured by the alkaline treatment or formed dispersed, nonsedimentable lipoprotein particles. In any case, the fact that RPE65 failed to remain soluble after pH adjustment or removal of the solubilizing agent argues against its classification as a peripheral membrane protein. We also showed that neither extremely hypotonic solutions nor 1 M hydroxylamine, pH 7.0, significantly released microsomal RPE65. As both treatments do release peripherally associated proteins anchored to membranes by palmitoylation, the RPE65-membrane

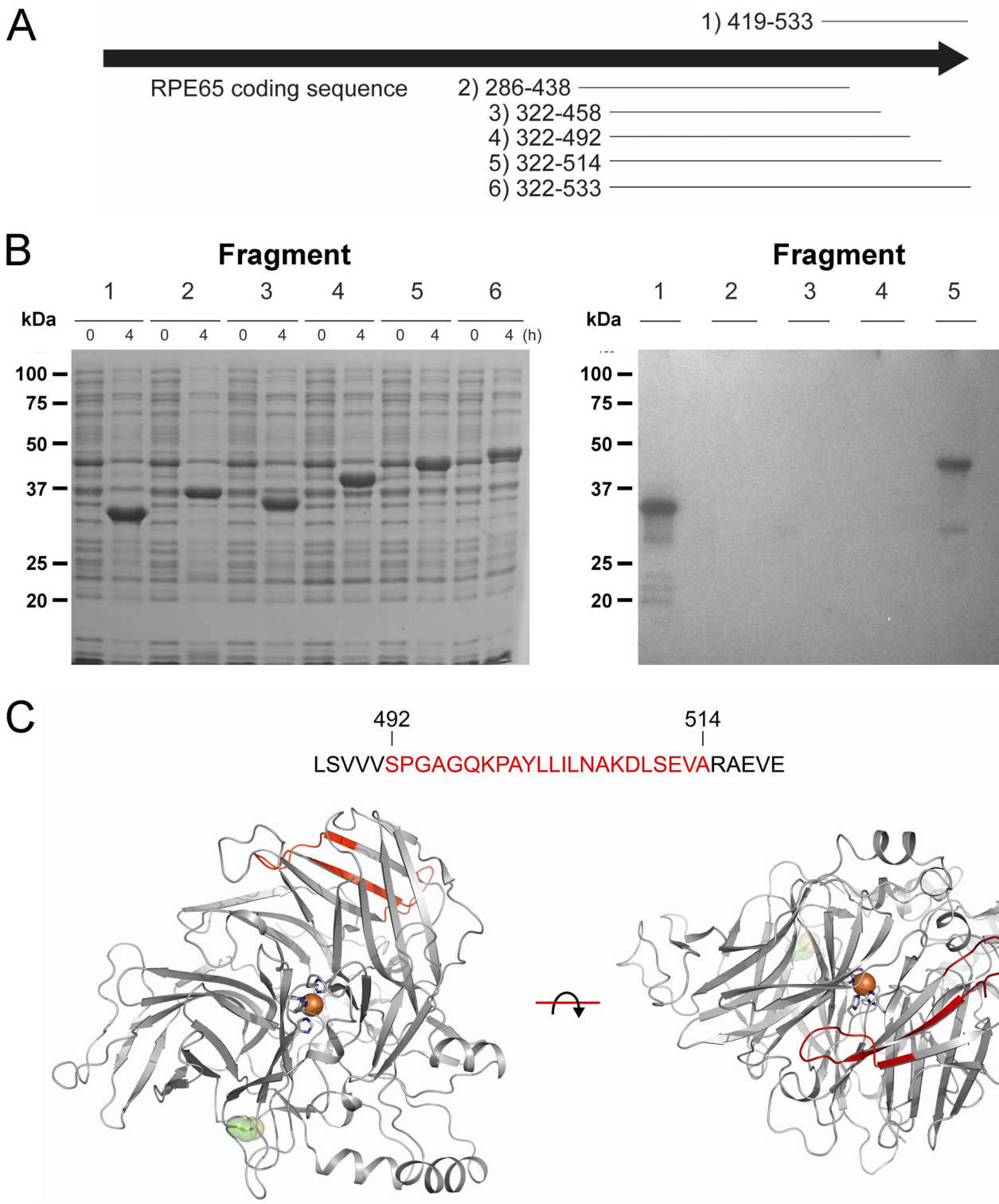

FIGURE 9. **Identification of the epitope-containing RPE65 segment recognized by an RPE65 monoclonal antibody.** *A,* outline of the strategy used to identify the epitope-containing segment. The *black arrow* represents the RPE65 coding region, and the *horizontal lines* indicate the region of the protein covered by each fragment. *Numbers* to the *left* of each *horizontal line* indicate the fragment number. *B,* expression and immunoblotting of the RPE65 fragments. Each of the RPE65 fragments was expressed as a thioredoxin fusion protein in *E. coli*. SDS-PAGE analysis of bacterial cell lysates with Coomassie stain (*left*) shows that after a 4-h induction with 1 mM isopropyl 1-thio-β-D-galactopyranoside, each fusion protein was expressed at a high level. Immunoblotting (*right*) of the bacterial lysates with RPE65 monoclonal antibody showed reactivity only with the fusion proteins containing RPE65 fragments 419–533, 322–514, and 322–533, consistent with the epitope residing within or immediately adjacent to residues 492–514. *C,* location of the epitope-containing region within the structure of RPE65. The amino acid sequence of the epitope-containing region is shown at the *top*. Location of the full or partial epitope-containing segment (colored *red*) within the tertiary structure of RPE65 is shown at the *bottom*. Orientation of the structure in the *left panel* is identical to that in Fig. 7. This structure is rotated 120° around the horizontal axis in the *right panel*. The epitope is found in a region of the protein predicted to face the cytosol and is located far from both the predicted membrane-binding face of the protein and the Cys-231 residue that cross-links with RDH5. This finding explains why the antibody is effective for both immunohistochemical studies and for purification of the RPE65-RDH5 cross-linked complex.

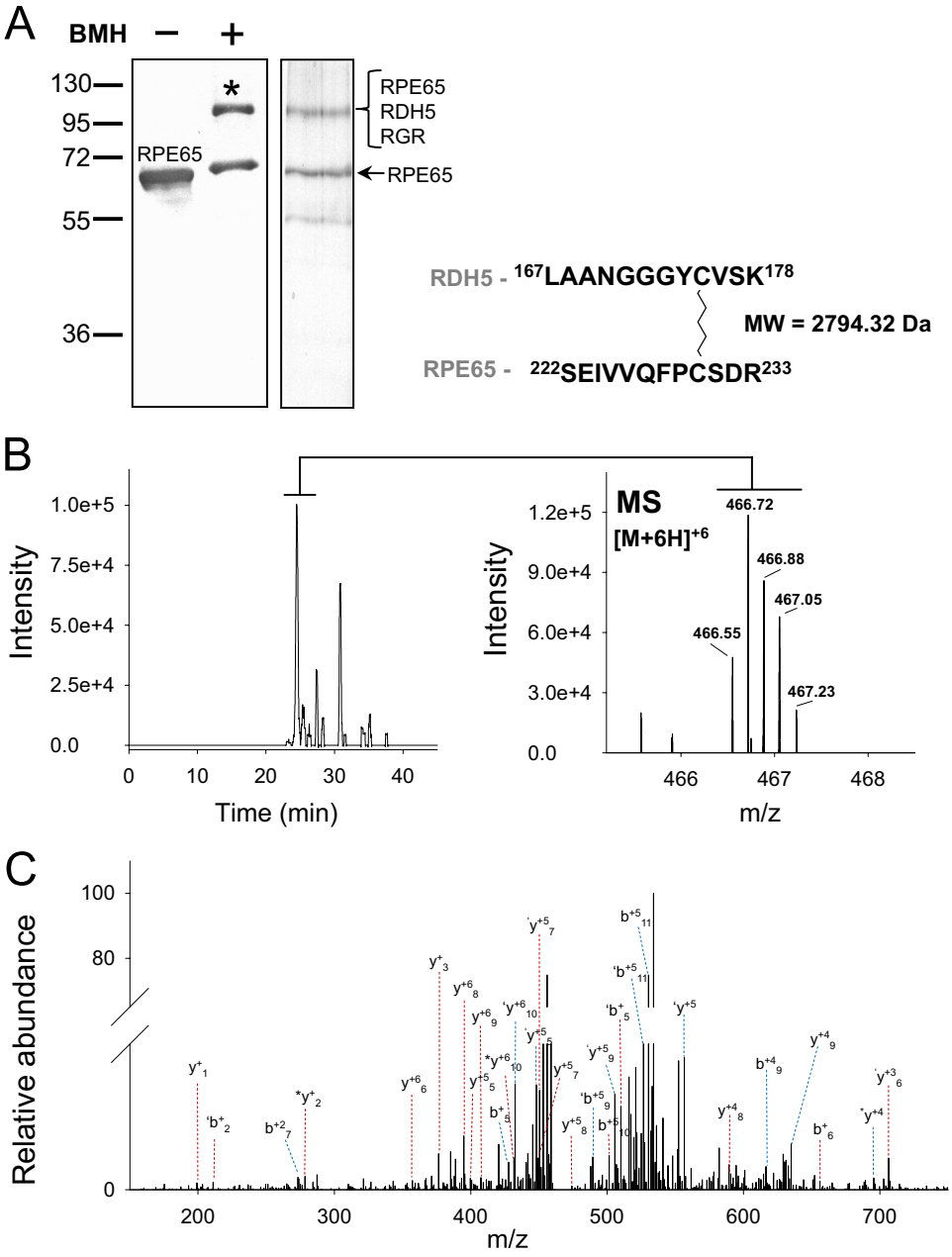

FIGURE 10. **Purification of the BMH-stabilized RPE65-containing complex and identification of its constituent proteins.** *A,* isolation of RPE65 and its complex was achieved on CNBr-activated Sepharose resin coupled to anti-RPE65 monoclonal antibody in the presence of 10 mM CHAPS in PBS. The purity of the preparation was verified by immunoblotting (*left panel*) and SDS-PAGE (*right panel*) revealing a highly purified sample. In-gel digest of a band corresponding to cross-linked RPE65 complex reveals the presence of two other lower molecular mass proteins (RDH5 and RGR) (Table 2). *B,* purified fractions were digested with trypsin, and the peptide composition was analyzed by mass spectrometry. The *left panel* shows the extracted ion chromatogram at $m/z = 466.7$ corresponding to a +6 ion (*right panel*) of intermolecularly cross-linked RPE65 and RDH5. *C,* amino acid sequence was confirmed based on this MS/MS spectrum of the 2794.3-Da peptide. Mass lines in the spectra that correspond to RPE65 and RDH5 sequences are colored in *red* and *blue*, respectively. Some of the most abundant identified ions are labeled with their respective fragment nomenclature.

interaction appears not to be solely attributable to this post-translational modification.

Instead we found that the nonionic detergent, C_8E_4 is highly effective for solubilizing microsomal RPE65. This suggests that interactions between amino acid side chains and the lipophilic membrane interior play a major role in the affinity of RPE65 for membranes. Consistent with this hypothesis and previous data (34, 35), we observed in Anapoe X-114 phase separation experiments that RPE65 was highly enriched in the detergent-rich phase, further demonstrating its integral membrane behavior.

These findings are all consistent with the recently determined crystal structure of RPE65 that reveals a large nonpolar surface surrounding the mouth of the tunnel that leads to the presumed catalytic center of the protein. One segment (residues 108–126), thought to contribute to membrane binding because of its amphiphilic character when modeled as an α-helix, was highly disordered in the original structure. To gain more structural information about this region, we collected a 1.9 Å dataset on a crystal that was isomorphous to those reported previously. But despite the improved resolution, we still did not observe stronger electron density for this missing segment indicating that it is intrinsically disordered in this crystal form.

A molecular packing analysis of hexagonal RPE65 crystals provides some insight into the surface of this protein that interacts with membranes. We observed that all RPE65 molecules in the unit cell are oriented such that the hydrophobic, putative membrane binding surface of RPE65 faces a large solvent channel in the crystal that runs parallel to the crystallographic 6_5 screw axis (Fig. 11). Given the strong interaction of RPE65 with nonionic detergent, it is quite likely that a protein-detergent mixed micelle was the building block of the crystal. Thus, we speculate that formation of the large solvent channel observed in the crystal was necessary to accommodate the associated detergent molecules. Indeed, similar packing arrangements have been observed in crystals of monotopic membrane proteins, such as prostaglandin H_2 synthases and squalene-hopene cyclase, that were crystallized in the presence of detergent (55).

A recent study by Ma and co-workers (36) that described the first successful reconstitution of RPE65 isomerization activity in phospholipid liposomes indicated that phospholipid membranes are of crucial importance for the enzymatic activity of RPE65. But because CHAPS, which strongly inhibits RPE65 activity, was used in this study, it remained unclear as to

TABLE 2

Proteins found in the BMH-cross-linked RPE65 complex

Affinity-purified, RPE65-containing cross-linked complexes were separated by SDS-PAGE. The peptides extracted from the Coomassie Blue-stained band corresponding to the BMH-stabilized RPE65 complex after in-gel digest were analyzed on an LTQ Orbitrap mass spectrometer. Peptides identified by Mascot with expected values of $p < 0.05$ and protein score >35 were included in the table.

Protein name	Accession number	Mass	No. of unique peptides	Sequence coverage
		Da		%
Membrane receptor p63 (RPE65)	gi564	60,932	13	24
11-*cis*-Retinol dehydrogenase	gi1054531	34,378	7	29
Retinal G protein-coupled receptor	gi28461177	31,940	4	17
Calnexin	gi157785567	67,750	2	5
Solute carrier family 3, member 2	gi59857795	63,182	2	4

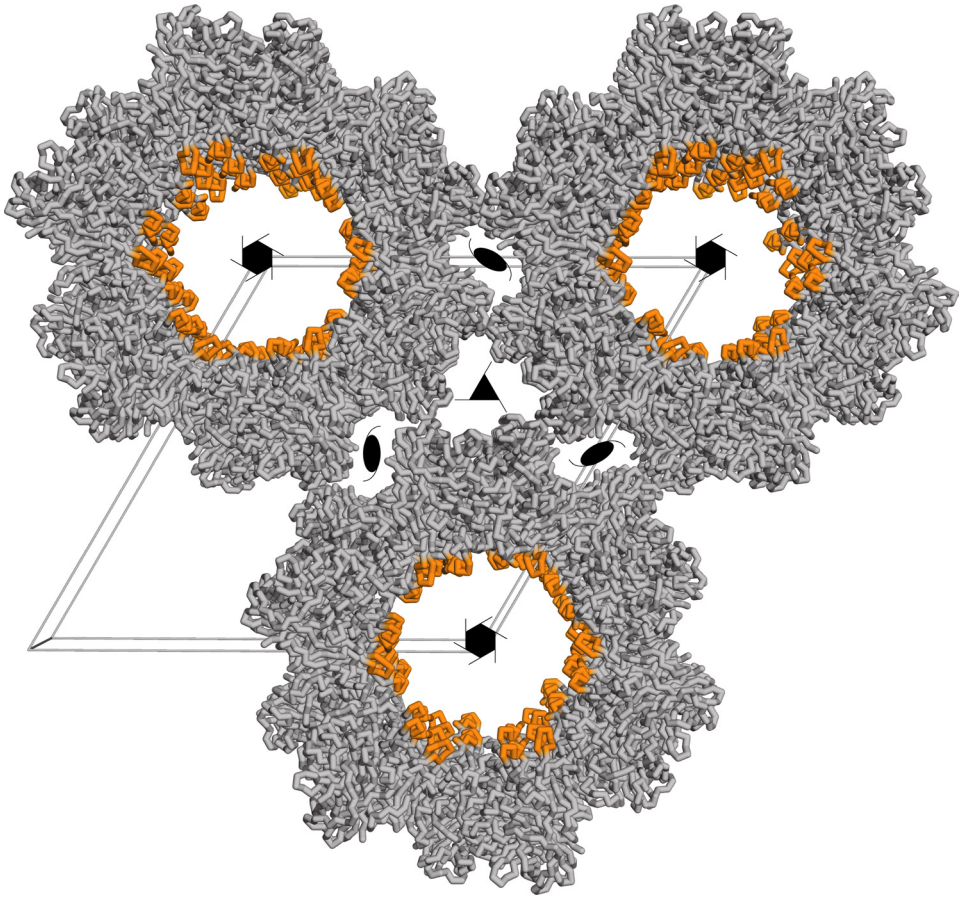

FIGURE 11. **Packing of RPE65 in the $P6_5$ unit cell.** The predicted membrane-binding face of RPE65 consisting of residues 196–202, 234–236, and 261–271 (colored *orange*) faces the largest solvent channel in the crystal. Based on the locations of residues 108 and 127, it is clear that the disordered but potentially amphiphilic segment, consisting of residues 109–126, also faces this channel. This packing arrangement may have been selected to accommodate a protein-detergent mixed micelle in the crystal, as has been noted for other monotopic membrane proteins. The *gray box* is an outline of a unit cell, and the *black symbols* indicate crystallographic symmetry elements. This figure was generated using PyMOL (Delano Scientific LLC, Palo Alto, CA) and Protein Data Bank code 3FSN.

whether the role of the membranes in the reconstituted assay was to provide a proper environment for extraction of lipophilic retinyl esters by the enzyme or to sequester CHAPS from the hydrophobic RPE65 active site so enzymatic activity would be restored.

In this study, strong evidence supporting a role for membrane phospholipid structure in maintaining retinoid isomerization activity stems from treatment of RPE microsomes with phospholipases. PLA_2-generated products of phospholipid hydrolysis can significantly influence mechanical properties of the lipid bilayer (56). Lysophospholipids induce membranes to form micellar structures, thereby generating a positive surface curvature. Positive bending strains are expected to loosen acyl chain packing, weaken lipid-lipid interactions near the membrane surface, and broaden headgroup spacing. These effects can be noted at lysophospholipid concentrations as low as 6% (molar) of total lipids. In many cases, including ion channels, enzymes, and phospholipases themselves, these changes in membrane properties have positive effects on enzymatic activity or folding of membrane proteins by improving diffusion rates or access to membrane-associated substrates (57–60). However, specific interactions of RPE65 with phospholipids made this enzyme susceptible to even small changes in lipid organization evoked by PLA_2 action. Surprisingly, hydrolysis of PC and PE did not cause detachment of RPE65 from the membrane. Unlike some peripherally bound enzymes, RPE65 has its active site deeply buried in a portion of the protein not predicted to interact with the membrane (24). Therefore, the substrate must be physically removed from the bilayer to undergo metabolism. If RPE65 were peripherally associated with the membrane through electrostatic interactions, for example, the extremely apolar substrate, all-*trans*-retinyl palmitate, would have to pass through the highly charged headgroup region of the bilayer to reach the active site, clearly an energetically unfavorable situation. By extending hydrophobic segments into the hydrophobic core of the bilayer, the protein provides both the elements needed to recognize the correct substrate among a variety of other membrane-dissolved small molecules and an energetically favorable passageway for substrate partitioning into the active site (61). Thus, a putative mechanism for enzyme deactivation may involve loss of the ability to access or pool retinyl esters from the lipid environ-

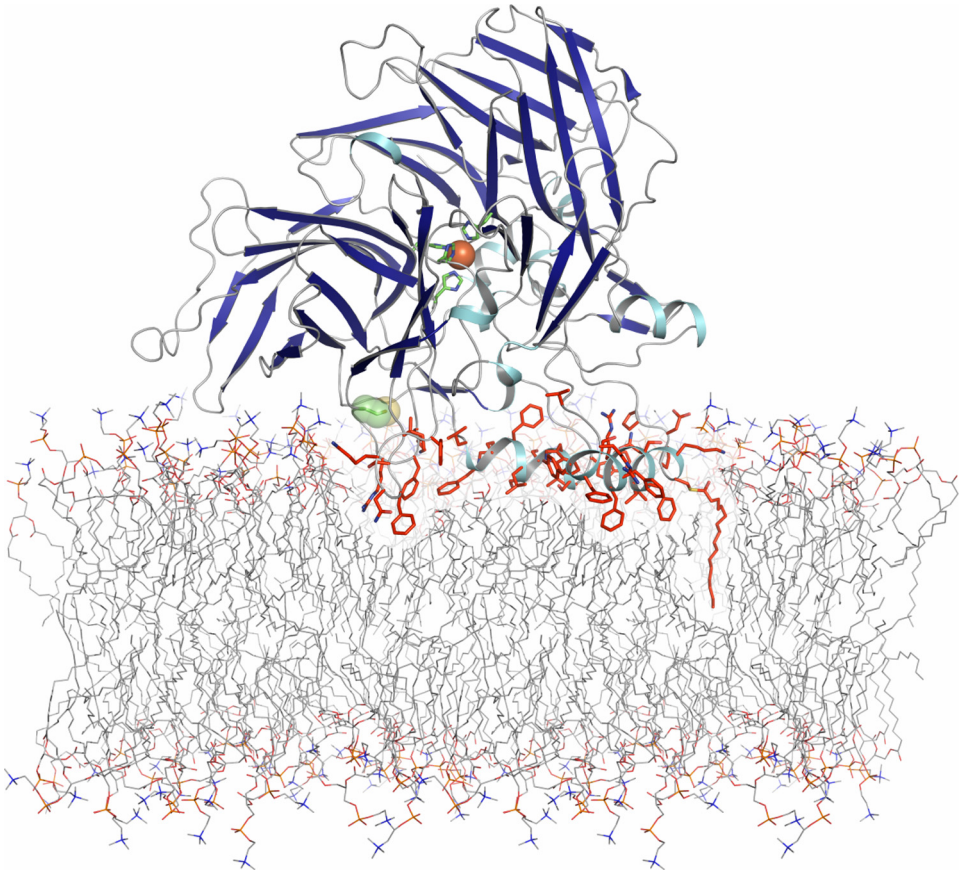

FIGURE 12. **RPE65 topology relative to a phosphatidylcholine bilayer.** Putative membrane-binding residues are colored *red*. A palmitoyl group identified by mass spectrometry is modeled on Cys-112. Residues 109–126, which could not be experimentally modeled because of weak electron density, are modeled as an α-helix in this figure as suggested by secondary structure prediction programs. The iron atom marking the RPE65 active site is shown as a *brown sphere*. Cys-231 identified as a cross-linking site is represented by *green* and *yellow spheres* indicating the position of the sulfhydryl group. This figure was generated using PyMOL (Delano Scientific LLC, Palo Alto, CA) and Protein Data bank entry 3FSN.

ment, most likely because of relaxation of residues involved in membrane binding, substrate recognition, and formation of the initial portions of the tunnel leading to the enzymatic active site. Indeed, in the RPE65 crystal structure, the putative residues involved in the aforementioned functions are by far the most mobile as indicated by their high *B*-factors. This observed high mobility may mimic what occurs in the loosened membrane structure produced by PLA_2 treatment.

As an alternative mechanism, RPE65 deactivation might relate to a reorganization of protein composition that occurs in RPE microsomes upon PLA_2 treatment. RPE65 was postulated to form a functional complex with other proteins involved in RPE retinoid metabolism including LRAT, CRALBP, RGR, and RDH5 (5, 62, 63). The last protein has been shown previously to co-purify and co-immunoprecipitate with native RPE65 (64, 65). Although a role of RDH5 in directly modulating RPE65 enzymatic activity has not been documented, this interaction might play a role in efficient transfer of retinoids between subsequent steps of the visual cycle, thereby increasing the rate of chromophore regeneration (66). Even though RPE65 was reported to fulfill a minimal requirement for detectable 11-*cis*-retinol production *in vitro*, co-expression of LRAT as a provider of all-*trans*-retinyl palmitate for the isomerization reaction *in situ* seems to be indispensable for robust enzymatic activity. In our studies, RPE microsomes were by far the richest source of retinoid isomerase activity compared with heterologously expressed RPE65. It is tempting to speculate that this discrepancy in 11-*cis*-retinol production may reflect differences in phospholipid composition and/or molecular (and subcellular) organization of the proteins involved in retinoid conversion. Clearly, perturbation of the phospholipid environment by PLA_2 treatment can modify microsomal membrane protein composition and limit the ability of RPE65 to interact with its putative protein partners, thereby reducing its enzymatic activity.

Identification of a pair Cys residues cross-linked by BMH provides insight into the putative orientation of interacting portions of RPE65 and RDH5 with respect to each other. BMH is a lipophilic reagent that easily partitions into phospholipid membranes. Thus, the observed modification of Cys-231 within the RPE65 primary sequence agrees well with the proposed topology of RPE65 based on its crystal structure that locates this residue at the membrane interface (Fig. 12) (24). Because structural data for RDH5 are not currently available, a homology model constructed on the basis of three-dimensional structures of guinea pig 11-β-hydroxysteroid dehydrogenase type I (11-β-HSD1) was used to determine the intermolecular location of Cys-175 that cross-linked to RPE65. In this model Cys-175 is found at the N terminus of helix F oriented perpendicular to and in close vicinity to the lipid membrane surface. This region was shown to form a short-chain dehydrogenase dimerization interface (64, 67). Because of this structural feature, efficient cross-linking between RPE65 and RDH5 may occur only with the monomeric form of retinol dehydrogenase. Interestingly, both RPE65 and RDH5 contain amphipathic helices, providing nonpolar surface contact with the hydrophobic core of the lipid bilayer characteristic for monotopic membrane proteins. Moreover, the RDH5 C-terminal helix provides an additional dimerization contact in 11-β-hydroxysteroid dehydrogenase type I and in the model. Hydrophobic interactions of these helices might assemble a putative contact surface between RPE65 and RDH5 in addition to RPE65 dimerization sites.

Data presented here may contribute to understanding certain physiological conditions. The rate of visual chromophore regeneration depends on the intensity of illumination *in vivo* and is 4-fold higher in the presence of moderately intense steady light as compared with dark conditions (63). However,

intense light exposure strongly reduces 11-*cis*-retinal production, as manifested by a reduced rate of rhodopsin regeneration in mice. Retinosomes within the RPE provide a dynamic retinoid storage system that rapidly accumulates all-*trans*-retinoids in the form of retinyl esters that are released from photoreceptors after light exposure (68). Thus, rapid LRAT-dependent biosynthesis of retinyl esters might be accompanied by a local, temporary depletion of PC and PE within phospholipid membranes, affecting RPE65 enzymatic activity as a consequence.

RPE65 is not the only example of a retinoid cycle protein that can be influenced by modifications in membrane composition (46). LRAT dimerization is also compromised by extensive phospholipid digestion. Interestingly, loss of its oligomeric state does not affect LRAT enzymatic activity because retinyl esters were still produced efficiently in the presence of synthetic diheptanoyl-PC. Thus, unexpectedly, PLA_2 treatment of RPE microsomes provides evidence suggesting that the monomeric form of LRAT is sufficient to sustain its catalytic properties.

In short, our study highlights the importance of phospholipid membrane structure for retinoid isomerization. Changes in phospholipid composition upon PLA_2 treatment are associated with progressive loss of 11-*cis*-retinol biosynthesis in RPE microsomes. The data suggest that this inhibitory effect is linked to an alteration in RPE65-membrane interactions and destabilization of a multiprotein RPE65 complex found in native RPE membranes. Thus, our data indicate the need for a proper lipid environment to maintain the enzymatic activity of RPE65. The observed tight binding of RPE65 to native microsomal membranes, its partitioning into the detergent-rich phase during Anapoe X-114 phase separation experiments, the functional dependence of RPE65 on proper structure of the membrane core, as well as the amphiphilic nature of the tertiary structure of this protein all indicate that RPE65 behaves largely as an integral monotopic membrane protein. Our findings contribute to a better understanding of a key step in the visual chromophore regeneration pathway.

Acknowledgments—We thank Dr. Janna Kiselar from the Center for Proteomics and Bioinformatics at Case Western Reserve University for assistance with MS instruments. We thank the staff at the APS 23-ID-D beamline for technical assistance. GM/CA CAT has been funded, in whole or in part, with federal funds from the National Cancer Institute (Y1-CO-1020) and the National Institute of General Medical Science (Y1-GM-1104). Use of the Advanced Photon Source was supported by the U.S. Department of Energy, Basic Energy Sciences, Office of Science, under Contract No. DE-AC02-06CH11357. We also thank Dr. Leslie T. Webster, Jr., and members of the Palczewski laboratory (Case Western Reserve University) for valuable comments about the manuscript.

REFERENCES

1. Palczewski, K. (2006) *Annu. Rev. Biochem.* **75,** 743–767
2. Travis, G. H., Golczak, M., Moise, A. R., and Palczewski, K. (2007) *Annu. Rev. Pharmacol. Toxicol.* **47,** 469–512
3. Jin, M., Li, S., Moghrabi, W. N., Sun, H., and Travis, G. H. (2005) *Cell* **122,** 449–459
4. Redmond, T. M., Poliakov, E., Yu, S., Tsai, J. Y., Lu, Z., and Gentleman, S. (2005) *Proc. Natl. Acad. Sci. U.S.A.* **102,** 13658–13663
5. Moiseyev, G., Chen, Y., Takahashi, Y., Wu, B. X., and Ma, J. X. (2005) *Proc. Natl. Acad. Sci. U.S.A.* **102,** 12413–12418
6. Redmond, T. M., Yu, S., Lee, E., Bok, D., Hamasaki, D., Chen, N., Goletz, P., Ma, J. X., Crouch, R. K., and Pfeifer, K. (1998) *Nat. Genet.* **20,** 344–351
7. Gu, S. M., Thompson, D. A., Srikumari, C. R., Lorenz, B., Finckh, U., Nicoletti, A., Murthy, K. R., Rathmann, M., Kumaramanickavel, G., Denton, M. J., and Gal, A. (1997) *Nat. Genet.* **17,** 194–197
8. Morimura, H., Fishman, G. A., Grover, S. A., Fulton, A. B., Berson, E. L., and Dryja, T. P. (1998) *Proc. Natl. Acad. Sci. U.S.A.* **95,** 3088–3093
9. Bereta, G., Kiser, P. D., Golczak, M., Sun, W., Heon, E., Saperstein, D. A., and Palczewski, K. (2008) *Biochemistry* **47,** 9856–9865
10. Moise, A. R., Golczak, M., Imanishi, Y., and Palczewski, K. (2007) *J. Biol. Chem.* **282,** 2081–2090
11. Zhang, M., Hu, P., and Napoli, J. L. (2004) *J. Biol. Chem.* **279,** 51482–51489
12. Saari, J. C., and Bredberg, D. L. (1990) *Methods Enzymol.* **190,** 156–163
13. Bordier, C. (1981) *J. Biol. Chem.* **256,** 1604–1607
14. Crabb, J. W., Chen, Y., Goldflam, S., West, K., and Kapron, J. (1998) *Methods Mol. Biol.* **89,** 91–104
15. Golczak, M., Maeda, A., Bereta, G., Maeda, T., Kiser, P. D., Hunzelmann, S., von Lintig, J., Blaner, W. S., and Palczewski, K. (2008) *J. Biol. Chem.* **283,** 9543–9554
16. Adamus, G., Zam, Z. S., Arendt, A., Palczewski, K., McDowell, J. H., and Hargrave, P. A. (1991) *Vision Res.* **31,** 17–31
17. Folch, J., Lees, M., and Sloane Stanley, G. H. (1957) *J. Biol. Chem.* **226,** 497–509
18. Baginski, E. S., Foà, P. P., and Zak, B. (1967) *Clin. Chem.* **13,** 326–332
19. Batten, M. L., Imanishi, Y., Maeda, T., Tu, D. C., Moise, A. R., Bronson, D., Possin, D., Van Gelder, R. N., Baehr, W., and Palczewski, K. (2004) *J. Biol. Chem.* **279,** 10422–10432
20. Kinter, M., and Sherman, N. E. (eds) (2000) *Protein Sequencing and Identification Using Tandem Mass Spectrometry,* pp. 147–164, Wiley-Interscience, New York
21. Wan, J., Roth, A. F., Bailey, A. O., and Davis, N. G. (2007) *Nat. Protoc.* **2,** 1573–1584
22. Xu, H., and Freitas, M. A. (2007) *BMC Bioinformatics* **8,** 133
23. Xu, H., Zhang, L., and Freitas, M. A. (2008) *J. Proteome Res.* **7,** 138–144
24. Kiser, P. D., Golczak, M., Lodowski, D. T., Chance, M. R., and Palczewski, K. (2009) *Proc. Natl. Acad. Sci. U.S.A.* **106,** 17325–17330
25. Otwinowski, Z., and Minor, W. (1997) *Methods Enzymol.* **276,** 307–326
26. Collaborative Computation Project, Number 4 (1994) *Acta Crystallogr. D* **50,** 760–763
27. Zwart, P. H., Grosse-Kunstleve, R. W., Lebedev, A. A., Murshudov, G. N., and Adams, P. D. (2008) *Acta Crystallogr. D* **64,** 99–107
28. Murshudov, G. N., Vagin, A. A., and Dodson, E. J. (1997) *Acta Crystallogr. D* **53,** 240–255
29. Emsley, P., and Cowtan, K. (2004) *Acta Crystallogr. D* **60,** 2126–2132
30. Davis, I. W., Leaver-Fay, A., Chen, V. B., Block, J. N., Kapral, G. J., Wang, X., Murray, L. W., Arendall, W. B., 3rd, Snoeyink, J., Richardson, J. S., and Richardson, D. C. (2007) *Nucleic Acids Res.* **35,** W375–W383
31. Yuan, Q., Kaylor, J. J., Miu, A., Bassilian, S., Whitelegge, J. P., and Travis, G. H. (2010) *J. Biol. Chem.* **285,** 988–999
32. Singer, S. J., and Nicolson, G. L. (1972) *Science* **175,** 720–731
33. Penefsky, H. S., and Tzagoloff, A. (1971) *Methods Enzymol.* **22,** 204–219
34. Hamel, C. P., Tsilou, E., Harris, E., Pfeffer, B. A., Hooks, J. J., Detrick, B., and Redmond, T. M. (1993) *J. Neurosci. Res.* **34,** 414–425
35. Båvik, C. O., Busch, C., and Eriksson, U. (1992) *J. Biol. Chem.* **267,** 23035–23042
36. Nikolaeva, O., Takahashi, Y., Moiseyev, G., and Ma, J. X. (2009) *FEBS J.* **276,** 3020–3030
37. Barry, R. J., Cañada, F. J., and Rando, R. R. (1989) *J. Biol. Chem.* **264,** 9231–9238
38. Tatulian, S. A. (2001) *Biophys. J.* **80,** 789–800
39. Chernomordik, L. (1996) *Chem. Phys. Lipids* **81,** 203–213
40. Stubbs, C. D., and Smith, A. D. (1984) *Biochim. Biophys. Acta* **779,** 89–137
41. Cooke, G. M., and Robaire, B. (1985) *J. Biol. Chem.* **260,** 7489–7495
42. Jensen, J. W., and Schutzbach, J. S. (1989) *Biochemistry* **28,** 851–855
43. Vesely, D. L. (1981) *Science* **213,** 359–360
44. Rydström, J. (1976) *Biochim. Biophys. Acta* **455,** 24–35

45. Katsuta, K., Tamai, Y., Watanabe, T., Fujita, S., and Satake, M. (1978) *Biochim. Biophys. Acta* **507,** 271–279
46. Jahng, W. J., Cheung, E., and Rando, R. R. (2002) *Biochemistry* **41,** 6311–6319
47. Bernstein, P. S., Law, W. C., and Rando, R. R. (1987) *Proc. Natl. Acad. Sci. U.S.A.* **84,** 1849–1853
48. Bernstein, P. S., Law, W. C., and Rando, R. R. (1987) *J. Biol. Chem.* **262,** 16848–16857
49. Hamel, C. P., Tsilou, E., Pfeffer, B. A., Hooks, J. J., Detrick, B., and Redmond, T. M. (1993) *J. Biol. Chem.* **268,** 15751–15757
50. Båvik, C. O., Lévy, F., Hellman, U., Wernstedt, C., and Eriksson, U. (1993) *J. Biol. Chem.* **268,** 20540–20546
51. Choo, D. W., Cheung, E., and Rando, R. R. (1998) *FEBS Lett.* **440,** 195–198
52. Takahashi, Y., Moiseyev, G., Ablonczy, Z., Chen, Y., Crouch, R. K., and Ma, J. X. (2009) *J. Biol. Chem.* **284,** 3211–3218
53. Ma, J., Zhang, J., Othersen, K. L., Moiseyev, G., Ablonczy, Z., Redmond, T. M., Chen, Y., and Crouch, R. K. (2001) *Invest. Ophthalmol. Vis. Sci.* **42,** 1429–1435
54. Xue, L., Gollapalli, D. R., Maiti, P., Jahng, W. J., and Rando, R. R. (2004) *Cell* **117,** 761–771
55. Wendt, K. U., Lenhart, A., and Schulz, G. E. (1999) *J. Mol. Biol.* **286,** 175–187
56. O'Regan, M. H., Alix, S., and Woodbury, D. J. (1996) *Neurosci. Lett.* **202,** 201–203
57. Booth, P. J. (2005) *Curr. Opin. Struct. Biol.* **15,** 435–440
58. Maingret, F., Patel, A. J., Lesage, F., Lazdunski, M., and Honoré, E. (2000) *J. Biol. Chem.* **275,** 10128–10133
59. Bell, J. D., Burnside, M., Owen, J. A., Royall, M. L., and Baker, M. L. (1996) *Biochemistry* **35,** 4945–4955
60. Burack, W. R., Gadd, M. E., and Biltonen, R. L. (1995) *Biochemistry* **34,** 14819–14828
61. Forneris, F., and Mattevi, A. (2008) *Science* **321,** 213–216
62. Mata, N. L., Moghrabi, W. N., Lee, J. S., Bui, T. V., Radu, R. A., Horwitz, J., and Travis, G. H. (2004) *J. Biol. Chem.* **279,** 635–643
63. Wenzel, A., Oberhauser, V., Pugh, E. N., Jr., Lamb, T. D., Grimm, C., Samardzija, M., Fahl, E., Seeliger, M. W., Remé, C. E., and von Lintig, J. (2005) *J. Biol. Chem.* **280,** 29874–29884
64. Simon, A., Hellman, U., Wernstedt, C., and Eriksson, U. (1995) *J. Biol. Chem.* **270,** 1107–1112
65. Hemati, N., Feathers, K. L., Chrispell, J. D., Reed, D. M., Carlson, T. J., and Thompson, D. A. (2005) *Mol. Vis.* **11,** 1151–1165
66. Jang, G. F., Van Hooser, J. P., Kuksa, V., McBee, J. K., He, Y. G., Janssen, J. J., Driessen, C. A., and Palczewski, K. (2001) *J. Biol. Chem.* **276,** 32456–32465
67. Ogg, D., Elleby, B., Norström, C., Stefansson, K., Abrahmsén, L., Oppermann, U., and Svensson, S. (2005) *J. Biol. Chem.* **280,** 3789–3794
68. Imanishi, Y., Batten, M. L., Piston, D. W., Baehr, W., and Palczewski, K. (2004) *J. Cell Biol.* **164,** 373–383